

CHAPTER I

INTRODUCTION

1.1 Rice¹

Rice (genus *Oryza*) is the most staple food for more than half of the world population. In Asia alone, more than 2,000 million people obtain 60-70 percent of their calories from rice and its products. Of 23 *Oryza* species, two are cultivated: *Oryza sativa*, which originated in the humid tropics of Asia, and *Oryza glaberrima* Steud, from West Africa. Asian cultivated rice has evolved into three eco-geographic race; *indica* (planted in tempera areas such as Southeast Asia and China), *japonica* (planted in Japan) and *javanica* (planted only in Indonesia).

Rice (*Oryza sativa* L.) is a short-lived plant related to the grass family, with a life cycle of 3-7 months. Rice can grow to 1–1.8 m tall, occasionally more depending on the variety and soil fertility. The grass has long, slender leaves 50–100 cm long and 2–2.5 cm broad. The small wind-pollinated flowers are produced in a branched arching to pendulous inflorescence 30–50 cm long. The edible seed is a grain (caryopsis) 5–12 mm long and 2–3 mm thick. The span of one cycle varies, depending on its type and the growing environment (see **Figure 1.1**).

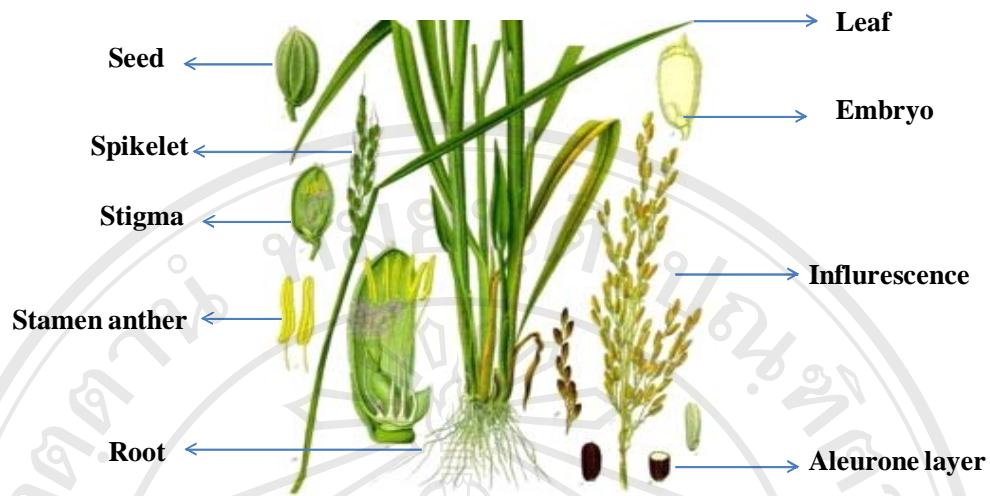


Figure 1.1 Schematic of rice.²

The growth of rice plant is divided into three phases:

1. Vegetative phase
2. Reproductive phase
3. Ripening phase

In the tropics, the reproductive phase is about 35 days and the ripening phase is about 30 days. The differences in growth duration are determined by changes in the length of the vegetative phase. These 3 growth phases consist of a series of 10 distinct stages. These stages are numbered and described as follows:

Stage 0: Germination to emergence

Stage 0 is from germination to emergence (see **Figure 1.2**). Seeds are usually pregerminated by soaking for 24 hours and incubating for another 24 hours. After pregerminations the radicle and plumule protrude through the hull. By the second or third day after seeding in the seedbed, the first leaf breaks through the coleoptiles. The end of stage 0 shows the emerged primary leaf (still curled) and an elongated radicle.

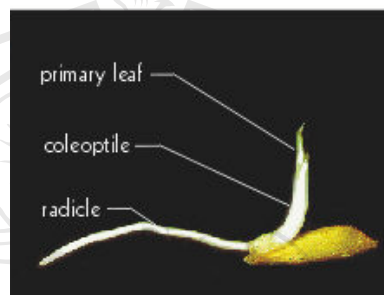


Figure 1.2 Germination to emergence stages of rice growth.

Stage 1: Seedling

Stage 1 is called seedling (see **Figure 1.3**). This stage starts right after emergence and lasts until just before the first tiller appears. During this stage, seminal roots and up to five leaves develop. As the seedling continues to grow, two more leaves develop. Leaves continue to develop at the rate of 1 every 3-4 days during the early stage. Secondary adventitious roots that form the permanent fibrous root system rapidly replace the temporary radical and seminal roots.

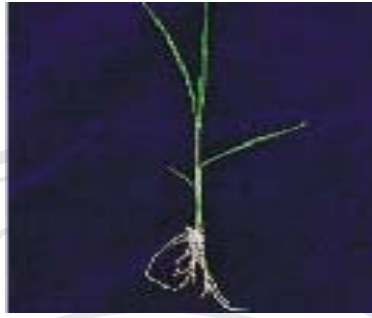


Figure 1.3 Seeding stage of rice growth.

Stage 2: Tillering

Stage 2 is called tillering (see **Figure 1.4**). This stage extends from the appearance of the first tiller until the maximum tiller number is reached. Tillers emerge from the auxiliary buds of the nodes and displace the leaf as they grow and develop.



Figure 1.4 Tillering stage of rice growth.

Stage 3: Stem elongations

Stage 3 is called stem elongation (see **Figure 1.5**). This stage may begin before panicle initiation or it may occur during the latter part of the tillering stage. Thus, there may be an overlap of stages 2 and 3. The tillers continue to increase in number and height, with no appreciable senescence of leaves noticeable. These first 4 stages make up the vegetative phase, the first phase of rice plant growth.

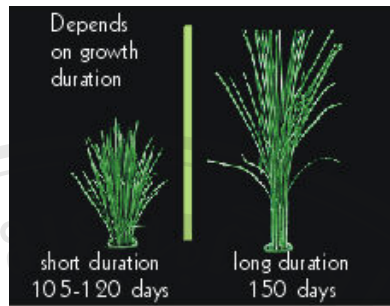


Figure 1.5 Stem elongations stage of rice growth.

Stage 4: Panicle initiations to booting

The initiation of the panicle primordium at the tip of the growing shoot marks the start of the reproductive phase (see **Figure 1.6**). The panicle primordium becomes visible to the naked eye about 10 days after initiation. At this stage, 3 leaves will still emerge before the panicle finally emerges. In short-duration varieties, the panicle becomes visible as a white feathery cone 1.0 -1.5 mm long. This bulging of the flag leaf sheath is called booting. Booting is most likely to occur first in the main culm.



Figure 1.6 Panicle initiations to booting stages of rice growth.

Stage 5: Heading or panicle exertion

Stage 5, heading, is marked by the emergence of the panicle tip from the flag leaf sheath (see **Figure 1.7**). The panicle continues to emerge until it partially or completely protrudes from the sheath.



Figure 1.7 Heading or panicle exsertion stages of rice growth.

Stage 6 flowering

Stage 6 is called flowering (see **Figure 1.8**). It begins when anthers protrude from the spikelet and then fertilization takes place. At flowering, the florets open, the anthers protrude from the flower glumes because of stamen elongation, and the pollen is shed. The florets then close. The flowering process continues until most of the spikelets in the panicle are in bloom.



Figure 1.8 Flowering stage of rice growth.

ลิขสิทธิ์มหาวิทยาลัยเชียงใหม่

Copyright© by Chiang Mai University

All rights reserved

Stages 4, 5, and 6 constitute the reproductive phase, the second phase of rice growth.

Stage 7: Milk grain stage

The last 3 stages of growth, stages 7, 8, and 9 comprise the ripening phase. In this milk grain stage, the grain has begun to fill with a milky material (see **Figure 1.9**). The grain starts to fill with a white, milky liquid, which can be squeezed out by pressing the grain between the fingers. The panicle looks green and starts to bend. Senescence at the base of the tillers is progressing. The flag leaves and the two lower leaves are green.



Figure 1.9 Milk grain stage of rice growth.

Stage 8: Dough grain stage

During this stage, the milky portion of the grain first turns into soft dough and later into hard dough (see **Figure 1.10**). The grains in the panicle begin to change from green to yellow. Senescence of tillers and leaves is noticeable. The field starts to look yellowish. As the panicle turns yellow, the last two remaining leaves of each tiller begin to dry at the tips.



Figure 1.10 Dough grain of rice growth.

Stage 9: Mature grain stage

In this stage, the individual grain is mature, fully developed, hard, and turned yellow (see **Figure 1.11**). The upper leaves are now drying rapidly although the leaves of some varieties remain green. A considerable amount of dead leaves accumulate at the base of the plant.



Figure 1.11 Mature grain stages of rice growth.

Stages 7 through 9 correspond to the ripening phase, the last phase in the development of the rice plant.³

Pigmented rice⁴

Pigmented rice (e.g. red, purple and black rice) are some variety of rice that have a color on the palea, lemma and another inside part such as pericarp tegmen and aleurone layer. The structure of the pigmented rice kernel is illustrated in **Figure 1.12**. These rice varieties have potential to promote human health because they contain antioxidative compounds that have the ability to inhibit the formation or to reduce the concentration of reactive cell-damaging free radicals. These compounds include flavonoids, anthocyanins, γ -oryzanols, vitamin E and phenolic compounds. Besides, it is well documented that consumption of pigmented rice bran can produce a hypocholesterolemic effect as well as antioxidant activity, attributed in major part to the presence of tocotrienols and γ -oryzanol.⁵ Feeding black rice to rodents in place of white rice has resulted in increased high density lipoprotein concentration in hypercholesterolemic rabbits, which corresponded to a reduction in the size of atherosclerotic lesions in these animals.⁶ A recent report showed that the supplementation of atherogenic diets with black rice pigment markedly reduced oxidative stress and inflammation in addition to modulating atherosclerotic lesions in the apolipoprotein E deficient mice. These findings indicate that compounds present in pigmented rice, which absent in white rice, provide cardiovascular protection in addition to the lipid-soluble components present in rice bran. Moreover, the recent study showed that pigmented rice varieties had greater antioxidant and free radical scavenging activities than non pigmented rice.

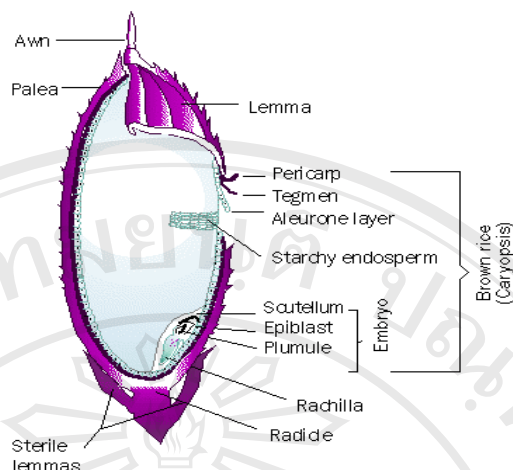


Figure 1.12 Schematic of the structure of pigmented rice kernel.⁷

Pigmented rice bran⁸ is the hard outer layer of grain and consists of combined aleurone and pericarp. Along with germ, it is an integral part of whole grains, and is often produced as a by-product of milling in the production of refined grains. When bran is removed from grains, they lose a portion of their nutritional value. Bran is present in and may be milled from any cereal grain, including rice, wheat, maize, oats, and millet. Bran is particularly rich in dietary fiber, and omegas and contains significant quantitative of starch, protein, vitamins, and dietary minerals.

Rice bran contains various antioxidants that impart beneficial effects on human health. It is well known that a major rice bran fraction contains 12%-13% oil and highly unsaponifiable components (4.3%). This fraction contains tocotrienols, γ -oryzanols, and β -sitosterol. All these constituents may contribute to the lowering of the plasma levels of the various parameters of the lipid profile. Rice bran also contains a high level of dietary fibers (β -glucan, pectin, and gum). In addition, it also contains 4-hydroxy-3-methoxycinnamic acid (ferulic acid), which may also be a component of the structure of non-lignified cell walls.⁹

Many researchers had reported the bioactive compounds of pigmented rice as shown by the studies below.

Zigoneanu and co-workers¹⁰ extracted rice bran oil by microwave-assisted extraction with isopropanol and hexane. The oil components were separated by normal-phase HPLC and quantified with a fluorescence detector. The radical scavenging capability of the oil was tested with DPPH assay.

Yawadio and co-workers¹¹ isolated two anthocyanins (cyanidin-3-*O*-glucoside and peonidin-3-*O*-glucoside) and other phenolics (ferulic acids) from black and pigmented brown rices (*Oryza sativa* L. *japonica*) and their complete structures were identified by spectroscopic analysis (H-NMR, C-NMR and MALDI-MS).

Chung and Shin¹² characterized alkaloids and phenolic acids from pigmented rice (*Oryza sativa* cv. *Heugjinjubyeo*). 4-Carboethoxy-6-hydroxy-2-quinolone, ethyl-3,4-dihydroxybenzoic acid, 4-hydroxy-3-methoxyphenylacetic acid, 3,4-dihydroxybenzoic acid, and 4-hydroxy-3-methoxy cinnamic acid were extracted from the ethyl acetate-soluble fraction of the aleurone layer of *Oryza sativa*. These compounds showed significant antioxidant activity.

Francisco and co-workers¹³ isolated the bioactive steroids from *Oryza sativa* L. Fifteen bioactive compounds were obtained and identified by spectroscopic methods. Eight of these compounds were obtained for the first time in *Oryza sativa*. They were β -sitosterol, 7-oxositosterol, stigmasterol, 7-oxostigmasterol, (6 α ,22E)-hydroxy-stigmata-4,22-dien-3-one, (6 β ,22E)-hydroxy-stigmata-4,22-dien-3-one, ergosterol peroxide, and 5 α ,8 α -pidioxy-24(R)-methylcolesta-6-en-3 β -ol. It was found that the most phytotoxic compounds on *E. Crus-galli* were ergosterol peroxide and 7-oxostigmasterol.

Ha and co-worker¹⁴ studied the bioactive components in rice bran oil which improved lipid profiles in rats fed a high-cholesterol diet. The liver cholesterol and triacylglycerol contents were higher in rats fed the high-cholesterol diet than the normal group but significantly decreased by bioactive components in rice bran oil supplementation. Similarly, hepatic thiobarbituric acid-reactive substances were increased by a high-cholesterol diet and reduced by bioactive components in rice bran oil supplementation in rats.

Imsanguana and co-workers¹⁵ compared the efficiency of three extraction methods: supercritical carbon dioxide extraction (SC-CO₂), solvent extraction and soxhlet extraction for extraction of α -tocopherol and γ -oryzanol from rice bran. The results showed that none of the solvents could extract α -tocopherol; however, ethanol was suitable for γ -oryzanol extraction. In summary, SC-CO₂ was found to be the best solvent for extracting both α -tocopherols and γ -oryzanols from rice bran, because it provided higher yields and extraction rate.

Kong and co-workers¹⁶ reported a high-performance capillary electrophoresis (CE) method with electrochemical detection (ED) for determination of myo-inositol and D-chiro-inositol in black rice bran. The linearity of two compounds were obtained in the concentration range from 1.0×10^{-16} to 1.0×10^{-14} g/ml and the detection limit was 5.3×10^{-7} and 7.3×10^{-7} g/ml for myo-inositol and D-chiro-inositol, respectively.

Youngmin Choi and co-workers¹⁷ determined antioxidant activity of the methanolic extracts from some grains and investigated relationships between antioxidant activities and antioxidant contents in the extracts. 2,2-Diphenyl-1-picrylhydrazyl radical (DPPH), ABTS, inhibitory lipid peroxidation, chelating activity and reducing power have been used to investigate the relative antioxidant activities of

the extracts from grains. The concentrations of total polyphenolics and carotenoids in the extracts were measured by spectrophotometry methods and vitamin E analysis was carried out by HPLC.

Shahid and co-workers¹⁸ studied the antioxidant properties and components of some commercially available varieties of rice bran. The order of antioxidant activity was evaluated by measurement of total phenolic content, antioxidant activity in linoleic acid system, reducing power, metal chelating ability, scavenging capacity by DPPH and ABTS cation radical and conjugated dienes. Determination of major antioxidant components reported in rice bran; tocopherols, tocotrienols and γ -oryzanol, were done using reversed phase HPLC.

1.2 Anthocyanins¹⁹

Phenolic compounds are important components of many fruits, vegetables, and beverages to which they contribute to flavor, color, and sensory properties such as bitterness and astringency. They are a wide range of compounds that possess an aromatic ring bearing hydroxyl substituent, including their functional derivatives such as esters, methyl esters, and glycoside. Flavonoids are the important class of phenolic compounds that found in food. They are C₁₅ compound (C₆-C₃-C₆) present as aglycone or in a glycoside form bound to various sugars, such as arabinose, glucose, galactose, rhamnose, and xylose. These polyphenols form a diverse range of compounds and can be classified into many classes (flavone, flavonol, flavonone, flavonol, anthocyanin, chalcone, isoflavanone and isoflavone) which are presented in

Figure 1.13.

Anthocyanins comprise a subgroup of flavonoids. They are present in nature mainly in the form of heterosides. The aglycon form of anthocyanins, also called anthocyanidin, is structurally based on the flavilium or 2-phenylbenzopyrilium ion (**Figure 1.14**), and possesses hydroxyl and methoxyl groups in different positions. Six anthocyanins (**Figure 1.15**) are commonly found in fruits and vegetables. The patterns of hydroxyl and methoxyl ion affect the color of anthocyanidins (**Table 1.1**).

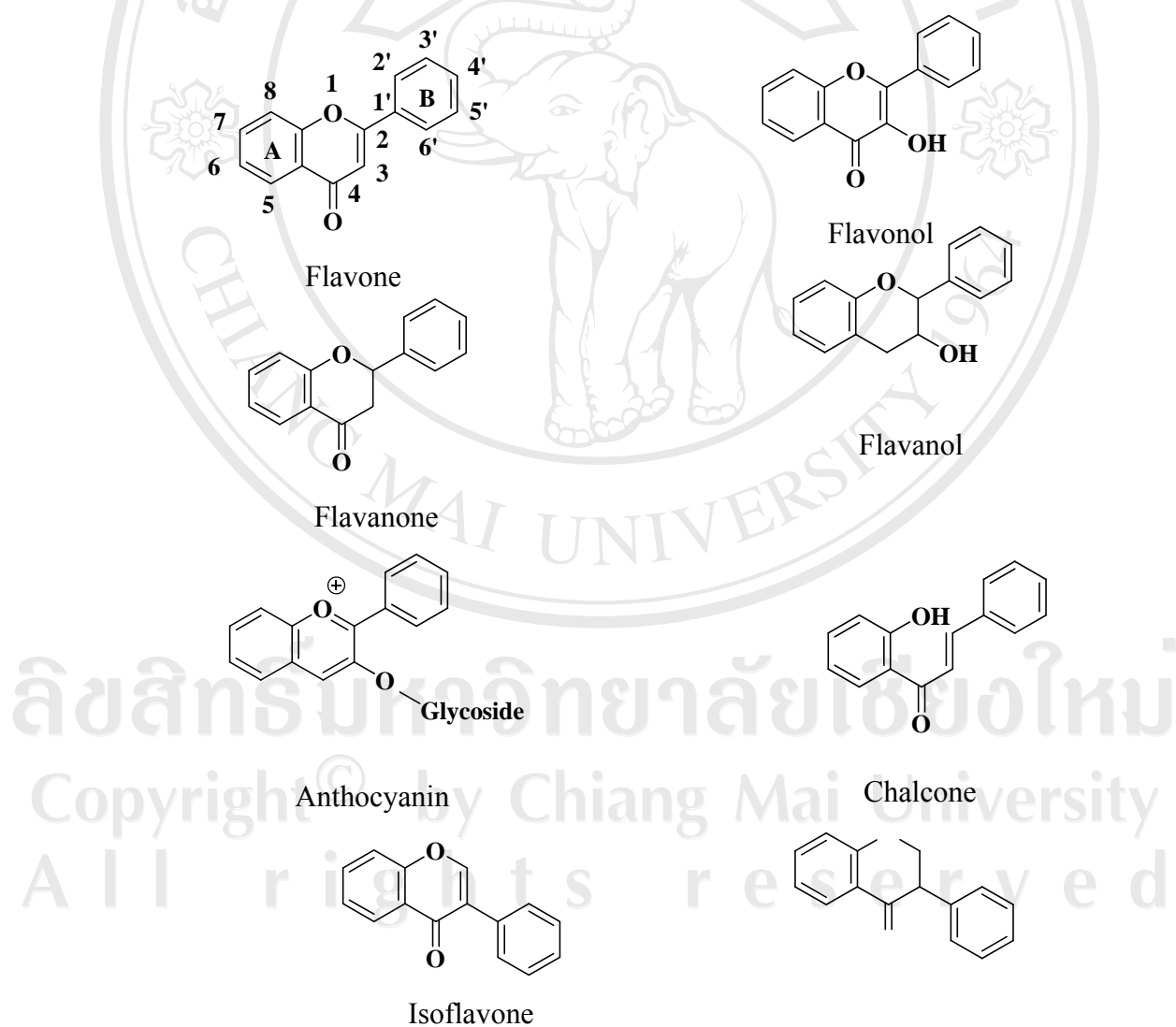


Figure 1.13 Basic structures of many classes of flavonoids.

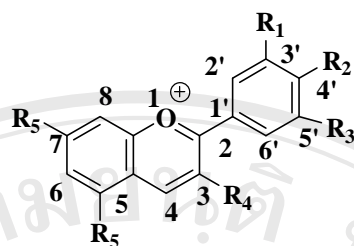


Figure 1.14 Basic structure of anthocyanidins.

Table 1.1 Naturally occurring anthocyanidins

Name	Substitution pattern							Color
	3	5	6	7	3'	4'	5'	
Apigenidin	H	OH	H	OH	H	OH	H	Orange
Auratinidin	OH	OH	OH	OH	H	OH	H	Orange
Cyanidin	OH	OH	H	OH	OH	OH	H	Orange-red
Delphinidin	OH	OH	H	OH	OH	OH	OH	Bluish-red
Europinidin	OH	OMe	H	OH	OMe	OH	OH	Bluish-red
Hirsutidin	OH	OH	H	OMe	OMe	OH	OMe	Bluish-red
Leteolinidin	H	OH	H	OH	OH	OH	H	Orange
Malvidin	OH	OH	H	OH	OMe	OMe	OMe	Bluish-red
Pelargonidin	OH	OH	H	OH	H	OH	H	Orange
Peonidin	OH	OH	H	OH	OMe	OH	H	Orange-Red
Petunidin	OH	OH	H	OH	OMe	OH	OH	Bluish-red
Puchellidin	OH	OMe	H	OH	OH	OH	OH	Bluish-red
Rosinidin	OH	OH	H	OMe	OMe	OH	H	Red

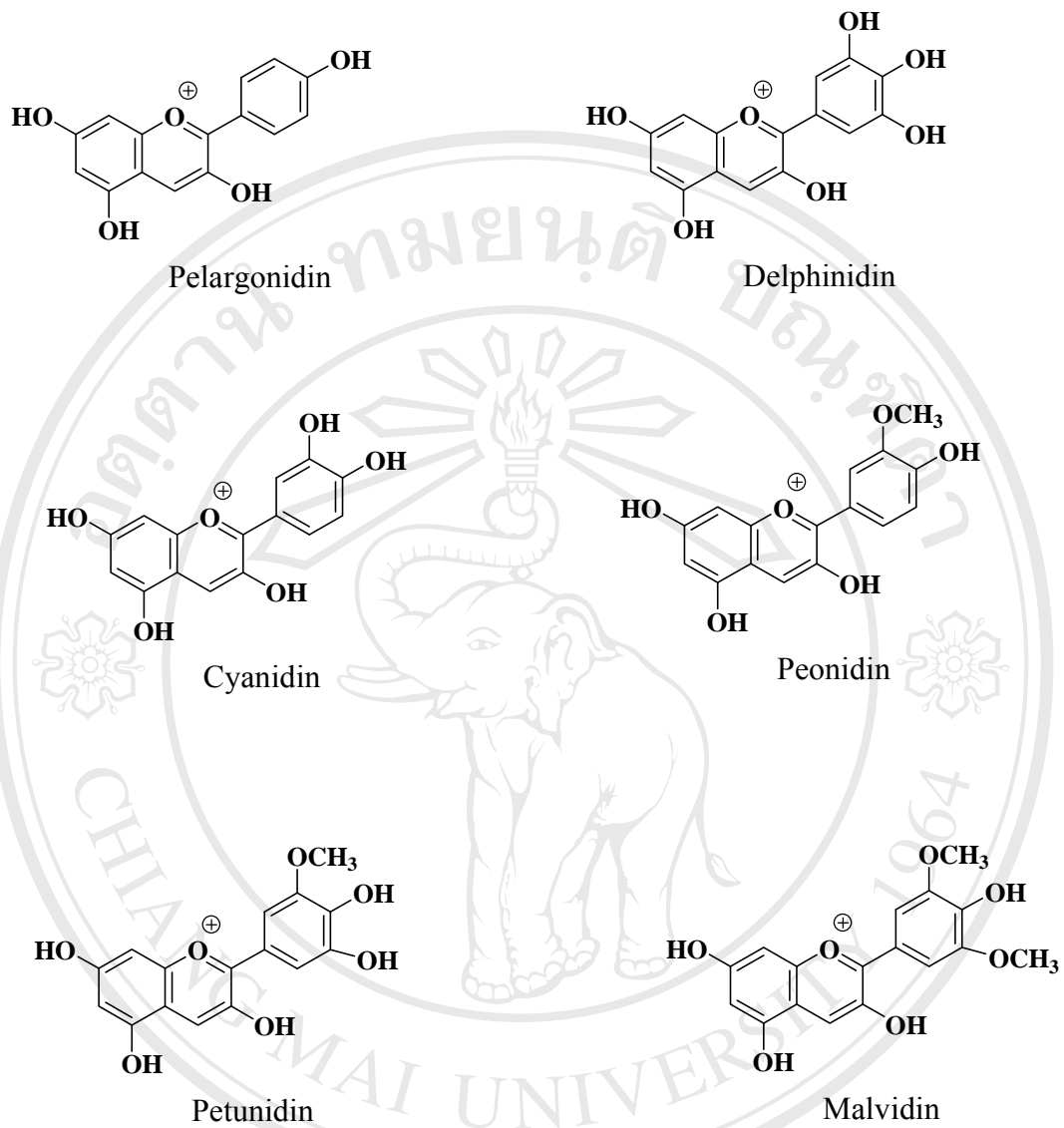


Figure 1.15 Structure of the anthocyanidins most commonly found in foods.

Over 250 naturally occurring anthocyanins have been identified, of which approximately 70 have been reported in fruits. The composition and content of anthocyanins allow difference of fruits from one another. These pigments are usually found in nature in the 3-monoglycoside, 3,5-diglucoside and acylglycoside of anthocyanins. However, glycosylated anthocyanins in positions 7, 3', 4', or 5' (**Figure 1.14**) may also occur. Presence of a second glycosyl group in anthocyanins brings about a characteristic bathochromic shift in their absorption maxima. This is used as mean for spectral differentiation of anthocyanins with a glycosyl group at position C-3 from those with a glycosyl group at position C-3 and position C-5. The sugar moiety can be glucose, arabinose, xylose, galactose, rhamnose, and fructose as well as rutinose (6-*O*- α -L-rhamnosyl-D-glucose), sorphorose (2-*O*- β -D-xylosyl-D-glucose), gentobiose (6-*O*- β -D-glucosyl-D-glucose), sambubiose (2-*O*- β -D-glucosyl-D-glucose), xylosylrutinose, and glucosylrutinose (see **Figure 1.16**).

Acylation of the sugar moiety of anthocyanins contributes to their color stability. Acylation usually occurs at the C-3 position of the sugar. Presence of two or more acyl group also increases the color stability of anthocyanin in aqueous solution.

The sugars usually are acylated with *p*-coumaryl, caffeic, ferulic, and sinapic acid (see **Figure 1.17**).

The stability of anthocyanins in plants is also associated with their ability to form complex with other phenolics, nucleic acids, sugars, amino acids, and metal ions such as calcium, magnesium, and potassium. The colored forms of anthocyanidins are stabilized by the presence of hydroxy group at the C-5 position and substitution at the C-4 position. This inhibits the addition of water and subsequent formation of colorless species. Moreover, the addition of methyl or phenyl group at C-4 position or the

conversion to deoxyanthocyanidins improves the stability of anthocyanins in the presence of sulfur dioxide or ascorbic acid.

Anthocyanins are very sensitive to change in pH. In solution, they exist in four different forms, neutral and ionized quinonoidal base, flavylium cation or oxonium salt, the colorless pseudobase and chalcone. The flavylium cation is weak acid, and a neutral quinonoidal base behaves as a weak acid and weak base. The distribution of these forms at equilibrium depends on pH and structure of anthocyanidins. The effect of pH on the predominant form of anthocyanin chromophore is given in **Figure 1.18**. Due to the equilibrium between flavylium cation and colorless carbinol structures, most intense red coloration of anthocyanins occurs in the pH ranges of 1-3.²⁰

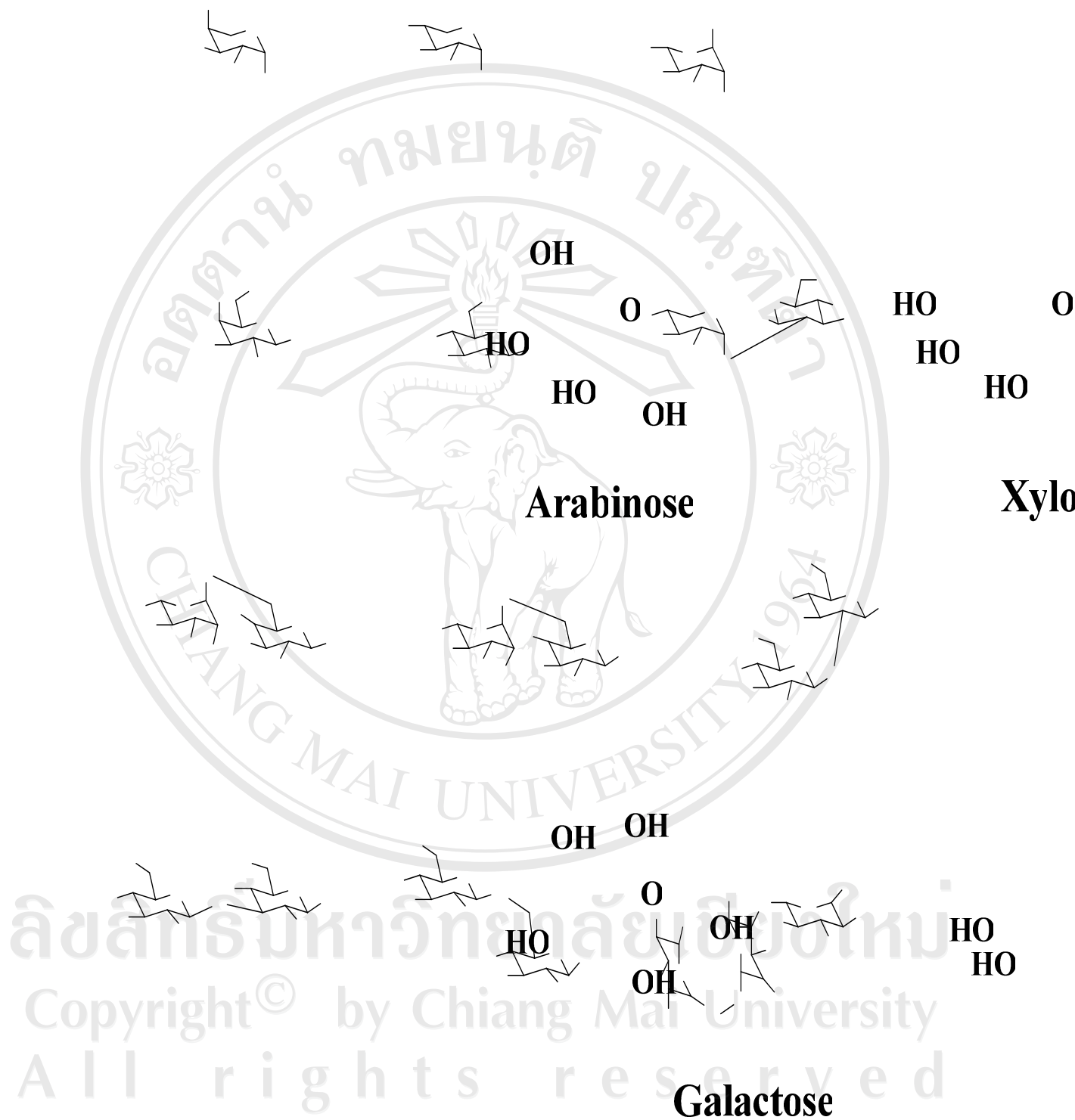


Figure 1.16 Chemical structures of many classes of sugar.

The beneficial pharmacological activities and biological properties of anthocyanins have been mainly attributed to their antioxidant properties, anticancer, antitumor, antimutagenic activity, anti-inflammatory, vasoprotective effects, beneficial effects in diabetes, the treatment of various ailments, including micro-circulation diseases, resulting from capillary fragility and the prevention of cholesterol-induced atherosclerosis.²¹

The antioxidant activity of anthocyanins is mainly due to their redox properties, which can play an important role in adsorbing and neutralizing free radical, quenching singlet and triplet oxygen, or decomposing peroxide. Crude extracts of fruits, herbs, vegetables, cereals, flowers and other plant materials rich in phenolics are increasing of interest in the food industry. The important of the antioxidant constituents of plant materials in the maintenances of health and protection from coronary heart disease and cancer is also raising interest.²²

Due to the effective and diverse functions of anthocyanins, which have been of interest to most researchers, several studies have emphasized on the identification and characterization of anthocyanins in vegetables, fruits, flowers, and other plants.

It was found that the major identified compounds were the glycosides, acylated-glycosides, and derivatives of anthocyanins as shown by the studies below.

In 1995, Farina and co-workers²³ analyzed anthocyanins in mallow flowers by HPTLC-densitometry in the reflectance mode at 530 nm and by reversed-phase HPLC. It was found that malvidin-3,5-*O*-diglucoside (malvidin) and malvidin-3-*O*-(6-*O*-malonylglucoside)-5-*O*-glucoside are components in the flower.

In 1996, Bridle and co-workers²⁴ identified anthocyanins in a red wine with elderberry extract. Cyanidin-3-sambubioside-5glucoside was found and the non-coloured phenolic detected in red wine were gallic acid, 3,4-dihydroxybenzoic acid, rutin, and quercetin.

In 1997, Bakker and co-workers²⁵ identified anthocyanin-type pigment, vitisin A, in small amounts in some red wines and at trace levels in stored grapes. Vitisin A was isolated, purified and identified using FAB-MS and NMR.

In 1998, Norbtek and Tado²⁶ investigated anthocyanins in the perianth segments of three cultivars of *crocus* by HPLC. Some novel anthocyanins were isolated from the blue flowers of *C. chrysanthus* and identified as petunidin-3-*O*-(6-*O*-malonyl-*D*-glucoside)-7-*O*-(6-*O*-malonyl-*D*-glucoside) and malvidin-3-*O*-(6-*O*-malonyl-*D*-glucoside)-7-*O*-(6-*O*-malonyl-*D*-glucoside). The anthocyanins isolated from the blue flowers of *C. sieberi* ssp. *Sublirnis*, were identified as 3,5-*D*-diglucosides of delphinidin and petunidin, and from *C. chrysanthus* were as their 3-rutinosides. The complete structural determination of each compound was achieved by use of one-dimensional and two-dimensional nuclear magnetic resonance spectroscopy techniques (1D and 2D NMR) and other spectral evidences.

In 1999, Torskangerpoll and co-workers²⁷ isolated the novel anthocyanin pelargonidin-3-*O*-[6-*O*-(2-*O*-acetyl- α -rhamnopyranosyl)-glucopyranoside] cyanidin-3-*O*-[6-*O*-(2-*O*-acetyl- α -rhamnopyranosyl)-glucopyranoside], pelargonidin-3-*O*-(6-*O*- α -rhamnopyranosyl-glucopyranoside), and cyanidin-3-*O*-(6-*O*- α -rhamnopyranosyl- β -glucopyranoside) in orange-red Tulipa *Queen Wilhelmina*. These structures were elucidated on the basis of chromatography, 1D NMR, 2D NMR and ESI-MS.

In 2000, Narayan and Venkataraman²⁸ isolated two anthocyanin pigments from cell cultures of carrot, Nentes scarlet 104 local variety. The chemical hydrolysis, column and paper chromatography, HPLC, ¹H and ¹³C NMR and MS studies indicated the presence of cyanidin-3-lathyroside [cyanidin-3-{xylopyranosyl-galactopyranoside}] and cyanidin-3-glucopyranoside in the callus cultures, whereas only cyanidin-3-lathyroside was found in carrot.

In 2001, Dugo and co-workers²⁹ identified anthocyanin components in some fruits such as black biberry, black berry and mulberry by narrow-bore HPLC-ESI-MS. UV-DAD and MS with ESI-source were used for detection. Fourteen anthocyanins in black biberry extract, six anthocyanins in black berry extract, and five anthocyanins in mulberry extract were identified.

In 2002, Fossen and co-workers³⁰ determined anthocyanin contents of 23 grass species (*Poaceae*). 3-(6-Malonylglucosides) and 3-glucosides of cyanidin, peonidin and delphinidin, 3-(3,6-dimalonylglucoside), 3-(6-rhamnosylglucoside) and 3-(6-glucosylglucoside) of cyanidin, in addition to peonidin-3-dimalonylglucoside and delphinidin-3-(6-rhamnosylglucoside) were identified. The 3-glucoside and 3-rutinoside of cyanidin were the major anthocyanins in *Sinarundinaria murielae* (subfamily Bambusoideae) and *Molinia caerulea* (subfamily Arundinoideae), while the 3-glucosides of cyanidin and peonidin were the principal anthocyanins in rice, *Oryza sativum* (subfamily Oryzoideae).

In 2003, Fossena and Olavstedal³¹ isolated the major anthocyanins from flowers of the orchids *Dracula chimaera* and *D. cordobae*. These compounds were cyanidin-3-*O*-(6-*O*-malonyl-glucopyranoside), cyanidin-3-*O*-(6-*O*-rhamnopyranosyl-glucopyranoside), cyanidin-3-*O*-glucopyranoside, peonidin-3-*O*-(6-*O*-

rhamnopyranosyl-glucopyranoside) and peonidin-3-*O*-(6-*O*-malonyl-glucopyranoside). The structures were characterized on the basis of 1D and 2D NMR spectroscopy, UV–Vis spectroscopy and MS.

In 2004, Villiersa and co-workers³² reported a rapid HPLC–DAD method for the routine analysis of 16 anthocyanins in wine. Malvidin-derived pigments were detected in red wine such as malvidin-3-glucoside, malvidin-acetyl-glucoside, malvidin-coumaroyl-glucoside, vitisin A, pinotin A, and pigment A.

In 2005, Tian and co-workers³³ reported HPLC coupled to PAD and ESI-MS/MS on a triple quadrupole techniques for investigation of the anthocyanin compositions of the purple-fleshed sweet potato (*Ipomoea batatas* L.) extract. Precursor ion analysis, product ion analysis, and selected reaction monitoring (SRM) MS/MS experiments were conducted sequentially to screen and characterize anthocyanins in the extract. Precursor ion analysis specifically detected the molecular cations of each category of anthocyanins by scanning the precursors of anthocyanidins (cyanidin, peonidin, and pelargonidin). The detected molecular cation of each anthocyanin was fragmented using product-ion analysis by collisionally activated dissociation (CAD). MS/MS using SRM detection was conducted to further confirm the fragmentation observed during product ion analysis. In comparison to the commonly used product-ion analysis technique, the combined use of precursor-ion analysis, product ion analysis, and SRM is particularly useful identification of anthocyanins in complex matrixes and provides important information to confirm the proposed structures. Twenty six anthocyanins were detected and characterized in the aqueous extract of the purple fleshed sweet potato (*Ipomoea batatas* L.).

In 2006, Longo and Vasapollo³⁴ extracted and identified anthocyanins from berries of *Smilax aspera* L. using by HPLC-DAD-MS. Pelargonidin-3-*O*-rutinoside represented about 83% of the total anthocyanin contents in the skin of *Smilax aspera* berries. A low quantity of cyanidin-3-*O*-rutinoside (13%) was also found.

In 2007, Latifolia and co-workers³⁵ extracted anthocyanin components in the berries of *Pistacia lentiscus* L., *Phillyrea latifolia* L. and *Rubia peregrina* L. The anthocyanins were extracted from the berries with 0.1% HCl methanol solution, purified on a C-18 solid-phase cartridge and characterized by HPLC-DAD-MS. The major anthocyanins of *P. lentiscus* berries were cyanidin-3-*O*-glucoside. The major anthocyanin in the extracts of *P. latifolia* and *R. peregrina* berries was cyanidin-3-*O*-rutinoside. Low quantities of cyanidin-3-*O*-glucoside have also been found.

In 2008, Duenas and co-workers³⁶ extracted the anthocyanin components in fig fruit (*Ficus carica* L.) from five different varieties (Colar, Cuello de Dama (green), Cuello de Dama (dark purple), Granilla and Bursa Siyahi). Fifteen anthocyanin pigments were detected. Cyanidin (Cy) as aglycone and some pelargonidin (Pg) derivatives were also found. Minor levels of peonidin-3-rutinoside (Pn-3-rutinoside) in the pulp were also detected. The pigment composition of the fig were anthocyanidin-derived pigments, namely 5-carboxypyranocyanidin-3-rutinoside, a cyanidin-3-rutinoside dimer and five condensed pigments containing C-C linked anthocyanins (Cy and Pg) and flavanol (catechin and epicatechin) residues.

Due to the large number of anthocyanins and their structural variations in closely related food, analytical procedures for the analysis of individual anthocyanins have been relatively difficult and complicated. Development of analytical methods

capable of high resolution separation of such anthocyanins as well as reducing steps for extraction is therefore important.

These analytical methods mostly employ a chromatographic technique with spectroscopic detection for both separation and identification of anthocyanins. Among various types of chromatographic technique available, the most widely used technique for analysis of anthocyanins is high performance liquid chromatography (HPLC) with mass spectrometric (MS) detection system.

1.3 Chromatography

The term chromatography embraces a family of closely related separation methods based on experiment described by Day and Tswett in 1897-1906. The feature distinguishing chromatography from most other physical and chemical methods of separation is that two mutually immiscible phase are brought into contact wherein one phase is stationary and the other mobile phase. The sample mixture, introduced into the mobile phase, undergoes a series of interaction (partitions) many times between the stationary phase and mobile phase as it is being carried through the system by the mobile phase. Interactions exploit difference in the physical or chemical properties of the components in the sample. These difference given the rate of migration of the individual components under the influence of the mobile phase moving through a column containing the stationary phase. Separated components emerge in the order of increasing interaction with the stationary phase. The least retarded component elutes first, the most strongly retained material elutes last. Separation is obtained when one component is retarded sufficiently to prevent overlap with the zone of an adjacent solute as sample components elute from the column.

Column is the heart of a chromatograph and provides versatility in the type of analyses that can be obtained with a single instrument. This versatility, due to the wide choice of material for the stationary and mobile phase, makes it possible to separate molecule that differ only slightly in their physical and chemical properties.

The mobile phase can be a gas or liquid, whereas the stationary phase can only be a liquid or solid. The fields of liquid column chromatography (LCC) embrace several distinct type of interaction. When the separation involves predominantly a simple partitioning between two immiscible liquid phases, one stationary and the other mobile phase, the process is call liquid-liquid (or partition) chromatography (LLC). When physical surface forces are mainly involved in the retentive ability of the stationary phase, the processes is denoted liquid-solid (or adsorption) chromatography (LSC). Two other chromatographic methods differ somewhat in their mode of action. In ion-exchange chromatography (IEC), ionic components of the sample are separated by selective exchange with counterion of the stationary phase. The use of exclusion packing as the stationary phase brings about a classification of molecules based largely on molecular geometry and size. Exclusion chromatography (EC) is referred to as gel permeation chromatography by polymer chemists and as gel filtration by biochemists. Finally, the mobile phase is a gas; the methods are called gas-liquid chromatography (GLC) and gas-solid chromatography (GSC).

1.3.1 High-performance liquid chromatography

High-performance liquid chromatography (HPLC) is a form of liquid chromatography to separate compounds that are dissolved in solution. HPLC instruments consist of a reservoir of mobile phase, a pump, an injector, a separation

column, and a detector. Compounds are separated by injecting a plug of the sample mixture onto the column. The different components in the mixture pass through the column at different rates due to differences in their partitioning behaviors between the mobile liquid phase and the stationary phase. Solvents must be degassed to eliminate formation of bubbles. The pumps provide a steady high pressure with no pulsating, and can be programmed to vary the composition of the solvent during the course of the separation. Detectors rely on a change in refractive index, UV-Vis absorption, or fluorescence after excitation with a suitable wavelength.³⁷ Diagram of high performance liquid chromatography is shown in **Figure 1.19**.

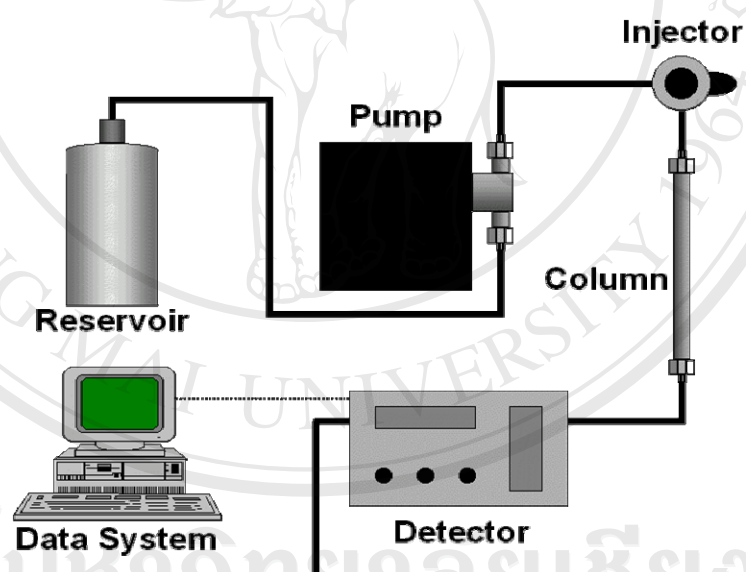


Figure 1.19 Diagram of high performance liquid chromatography (HPLC).³⁸

1.3.1.1 Types of HPLC

1.3.1.1.1 Normal phase chromatography (NP-HPLC)

Normal phase chromatography was the first kind of HPLC chemists used. It separates analytes based on polarity. This method uses a polar stationary phase and a non-polar mobile phase, and is used when the analyte of interest is fairly polar in nature. The polar analyte associates with and is retained by the polar stationary phase. Adsorption strengths increase with increase in analyte polarity, and the interaction between the polar analyte and the polar stationary phase (relative to the mobile phase) increases the elution time. The interaction strength not only depends on the functional groups in the analyte molecule, but also on steric factors and structural isomers are often resolved from each another. Use of more polar solvents in the mobile phase will decrease the retention time of the analytes while more hydrophobic solvents tend to increase retention times. Particularly polar solvents in a mixture tend to deactivate the column by occupying the stationary phase surface. This is somewhat particular to normal phase because it is most purely an adsorptive mechanism (the interactions are with a hard surface rather than a soft layer on a surface)

1.3.1.1.2 Reversed phase chromatography

Reversed phase HPLC (RP-HPLC) consists of a non-polar stationary phase and an aqueous, moderately polar mobile phase. One common stationary phase is silica which has been treated with RMe_2SiCl , where R is a straight chain alkyl group such as $\text{C}_{18}\text{H}_{37}$ or C_8H_{17} . The retention time is therefore longer for molecules which are more non-polar in nature, allowing polar molecules to elute more readily. Retention

time is increased by the addition of polar solvent to the mobile phase and decreased by the addition of more hydrophobic solvents.

1.3.1.1.3 Size exclusion chromatography

Size exclusion chromatography (SEC), also known as *gel permeation chromatography* or *gel filtration chromatography*, separates particles on the basis of size. It is generally a low resolution chromatography and thus it is often reserved for the final, "polishing" step of purification. It is also useful for determining the tertiary structure and quaternary structure of purified proteins. This technique is widely used for the molecular weight determination of polysaccharides. SEC is the official technique for the molecular weight comparison of different commercially available low-molecular weight heparins.³⁹

1.3.1.1.4 Ion exchange chromatography

In ion-exchange chromatography, retention is based on the attraction between solute ions and charged sites bound to the stationary phase. Ions of the same charge are excluded. Some types of ion exchangers include: (1) Polystyrene resins allows cross linkage which increases the stability of the chain. Higher cross linkage reduces swerving, which increases the equilibration time and ultimately improves selectivity. (2) Cellulose and dextran ion exchangers (gels). These possess larger pore sizes and low charge densities making them suitable for protein separation. In general, ion exchangers favor the binding of ions of higher charge and smaller radius. An increase in counter ion (with respect to the functional groups in resins) concentration reduces the retention time. An increase in pH reduces the retention time in cation exchange

while a decrease in pH reduces the retention time in anion exchange. This form of chromatography is widely used in the following applications; purifying water, preconcentration of trace components, ligand-exchange chromatography, ion-exchange chromatography of proteins, high-pH anion-exchange chromatography of carbohydrates and oligosaccharides, etc.

The variety of detection mode available for HPLC analyses that provide additional information about the eluent as it exist the column greatly facilitates unknown characterizations. The major of analytical methods for phenolic compounds includes HPLC with spectrophotometer-based detection techniques (UV absorption, fluorescence, and photo diode array), electrochemical detection, and HPLC with mass spectrometry.⁴⁰

1.3.2 HPLC-UV absorption

The UV-VIS absorption detector consists of a source, a wavelength selection device, a sensor (see **Figure 1.20**). The source emits radiation in the UV-Vis region of the spectrum. The wavelength selection device isolates and passes the appropriate wavelength(s) from the source and rejects the rest of the light. The wavelength selection device may precede the sample as indicated or it may follow it. The sensor responds to the transmitted light and generates a measurable electrical signal.

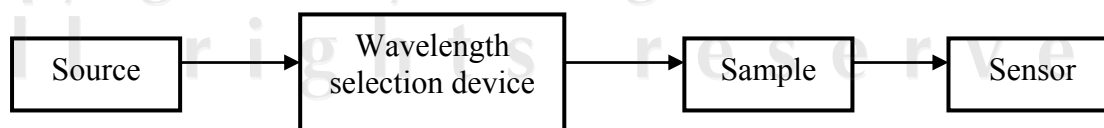


Figure 1.20 A schematic diagram of UV-Vis absorption detector.

Anthocyanin components absorb well in the UV region, and the most commonly used detector for HPLC is a variable-wavelength UV-detector. This detector offers a high degree of sensitivity and is capable of collecting data of one or more wavelength simultaneously. No single wavelength is ideal for monitoring all classes of phenolics, since they display absorbance maxima at different wavelengths. For maximum sensitivity, usually a wavelength near the maxima is desired; however, in practice, since absorption maxima can differ greatly between compounds, wavelengths are set for the best overall detection of all components.

1.3.3 HPLC-fluorescence

Fluorescence detectors are also used for anthocaynins but have not been applied widely to the detection of LC system.

1.3.4 HPLC-photo diode array

Spectrophotometers were improved somewhat by dual-wavelength detectors (**Figure 1.21**), but it was not until the development of the photodiode array (PDA) that spectrophotometer techniques were revolutionized. The photodiode array detectors, which can acquire data in both time and spectral domain, has led to considerable improvements in HPLC food analysis for the purpose of identification and has demonstrated the usefulness of qualitative information in anthocyanins analysis based on the absorption spectrum.

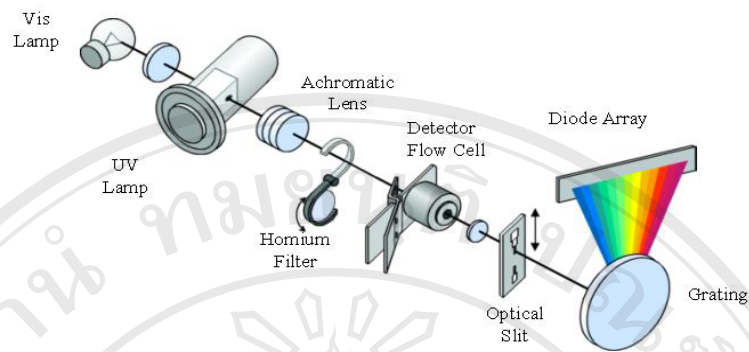


Figure 1.22 A schematic of photo diode array detector diagram.⁴¹

Photodiode array detection has three major advantages for HPLC analysis as followings:

- multiple wavelength detection
- peak identification
- peak-purity determination

Since PDA can record the characteristic UV spectra of the different anthocyanins when they were eluted from the column. Characterization and peak-purity information can be facilitated through comparisons of the spectra at the front, the apex, and the tail of each peak. A PDA can be employed to obtain spectral data and to study further some structural features, such as functional group conjugated with aromatic ring, degree of substitution, and position of unknown peaks of anthocyanins. Anthocyanins consist of structurally similar compounds, typically differing only in the degree of ring substitution, the type of substitution (hydroxyl,

methoxyls, etc.), and the type and degree of glycosylation. Thus, the addition of a second hydroxyl group to the basic structure has little effect on their spectra by PDA.

1.3.4 HPLC-electrochemical detection

HPLC-based electrochemical detection (HPLC-ECD) is very sensitive for those compounds that can be oxidized or reduced at low voltage potentials. Spectrophotometer-based HPLC techniques (UV absorption and Fluorescence) measure a physical property of molecule. Electrochemical detection, however, measures a compound by actually changing it chemically. The ECD is becoming increasingly important for determination of very small amounts of phenolics, as it provides enhanced sensitivity and selectivity. Electrochemical detection offers the advantage of superior sensitivity and selectivity over other HPLC detectors, which is very useful when analyzing real samples, reducing matrix effects, and consequently improving the identification of the analyst peaks. Furthermore, ECD is almost insensitive to the changes in mobile phase condition associated with gradient elution.⁴²

1.3.5 HPLC-mass spectrometry

Mass spectrometry is an analytical technique that measures the mass-to-charge ratio (m/z) of charged particles. It is most generally used to find the composition of a physical sample by generating a mass spectrum representing the masses of sample components. The mass spectrum is measured by a mass spectrometer.

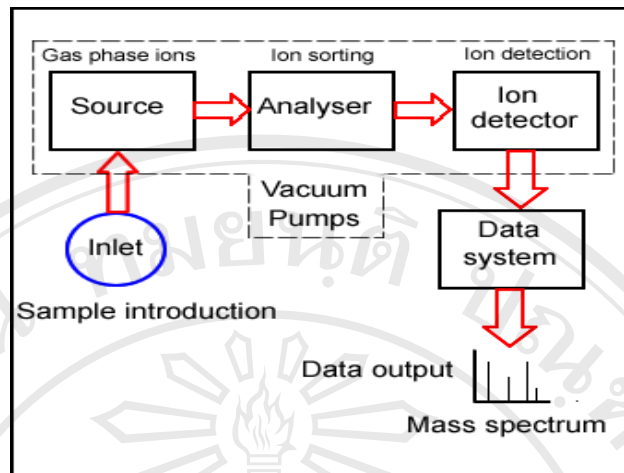


Figure 1.22 Schematic diagram of a mass spectrometer.⁴³

Mass spectrometers consist of three basic parts: an ion source, a mass analyzer, and a detector system (**Figure 1.22**). The stages within the mass spectrometer are:

1. Production of ions from the sample.
2. Separation of ions with different masses.
3. Detection of the number of ions of each mass produced.
4. Collection of data to generate the mass spectrum.

The technique is applicable in:

- identifying unknown compounds by the mass of the compound molecules or their fragments
- determining the isotopic composition of elements in a compound
- determining the structure of a compound by observing its fragmentation

- quantifying the amount of a compound in a sample using carefully designed methods (mass spectrometry is not inherently quantitative)
- studying the fundamentals of gas phase ion chemistry (the chemistry of ions and neutrals in vacuum)
- determining other important physical, chemical, or even biological properties of compounds with a variety of other approaches.

Different chemicals have different masses, and this fact is used in a mass spectrometer to determine what chemicals are present in a sample. For example, table salt (NaCl), may be vaporized (turned into gas) and ionized (broken down) into electrically charged particles (Na^+ and Cl^-), called ions, in the first phase of the mass spectrometry. The sodium ions are monoisotopic, with mass 23Da. Chloride ions have two isotopes of mass 35 Da (~75%) and mass 37 Da (~25%). They also have a charge, which means that the speed and direction may be changed with an electric or magnetic field. An electric field accelerates the ions to a high speed. After this, they are directed into a magnetic field which applies a force to each ion perpendicular to the plane defined by the particles direction of travel and the magnetic field lines. This force deflects the ions (makes them curve instead of traveling in a straight line) to varying degrees depending on their m/z . Lighter ions get deflected more than the heavier ions. This can be explained by Newton's second law of motion. The acceleration of a particle is inversely proportional to its mass. Therefore, the magnetic field deflects the lighter ions more than it does the heavier ions. The detector measures the deflection of each resulting ion beam. From this measurement, the m/z

of all the ions produced in the source can be determined. From this information, the chemical composition of the original sample (i.e. that both sodium and chlorine are present in the sample) and the isotopic compositions of its constituents (i.e. whether the ratio of ^{35}Cl to ^{37}Cl has been changed by some process) can be determined. Techniques for ionization have been key to determining what types of samples can be analyzed by mass spectrometry. Electron ionization and chemical ionization are used for gases and vapors. In chemical ionization sources, the analyte is ionized by chemical ion-molecule reactions during collisions in the source. Two techniques often used with liquid and solid biological samples include electrospray ionization and matrix-assisted laser desorption-ionization (MALDI). Inductively coupled plasma sources are used primarily for metal analysis on a wide array of sample types. Others include glow discharge, field desorption (FD), fast atom bombardment (FAB), thermospray, desorption-ionization on silicon (DIOS), direct analysis in real time (DART), atmospheric pressure chemical ionization (APCI), secondary ion mass spectrometry (SIMS), spark ionization and thermal ionization. Ion attachment ionization is a newer soft ionization technique that allows for fragmentation free analysis.⁴⁴

Fast atom bombardment (FAB)

There are a number of fast particle beam desorption ionization methods. Fast particle desorption ionization superseded the earlier field desorption method, which always suffered from complex source design and sample preparation. The techniques of FAB is very similar in concept and design as they both involve the bombardment of a solid spot of the analyte-matrix mixture on the end of a sample probe by a fast

particle beam (see **Figure 1.23**). The matrix (a small organic species like glycerol or 3-nitrobenzyl alcohol) is used to keep a homogenous sample surface. The particle beam is incident onto the surface of the analyte-matrix spot, where it transfers its energy bringing about localized collisions and disruptions. Some species are ejected (sputtered) from the surface as secondary ions by this process. These ions are then extracted and focused before passing to the mass analyzer. The polarity of ions produced depends on the source potentials. **Figure 1.23** shows a positive ion beam being formed.

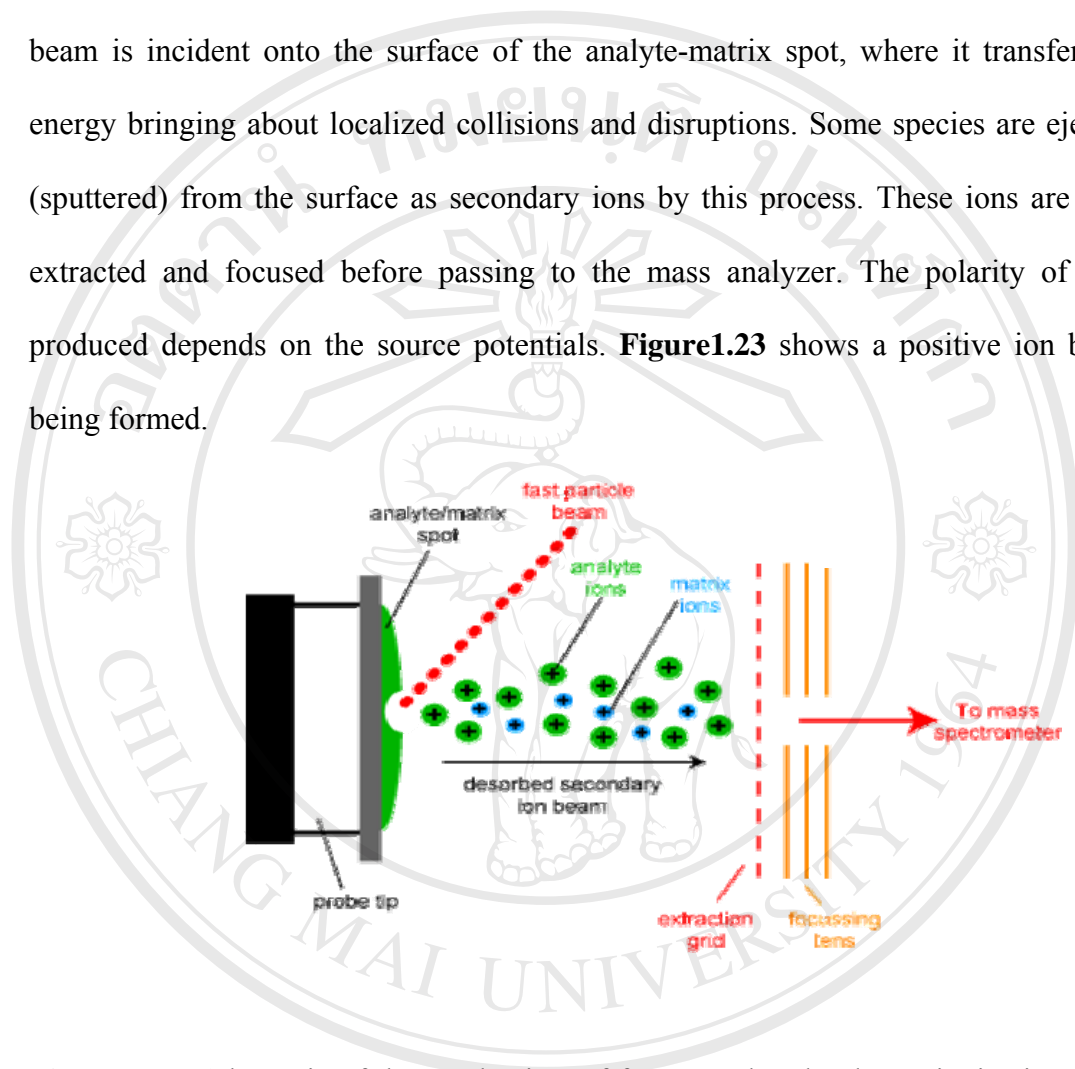


Figure 1.23 Schematic of the mechanism of fast atom bombardment ionization mass spectrometry (FAB).⁴⁵

MALDI mass spectrometry

MALDI mass spectrometry was demonstrated that the irradiation of low-mass organic molecules with a high-intensity laser pulse lead to the formation of ions that could be successfully mass analyzed. This was the origins of laser desorption (LD) ionization. Other the next few decades, the technique underwent substantial

development, culminating in the extension of the technique to the volatilizations of non-volatile biopolymers and organic macromolecules. There was, however, a sharp cut of in mass at about 5-10 kDa, limiting the technique's application. The other main limitation was that ions were created in bursts which prevented the technique from being coupled to scanning mass analyzers. In fact LD was only really successful when coupled to TOF-mass analyzers.

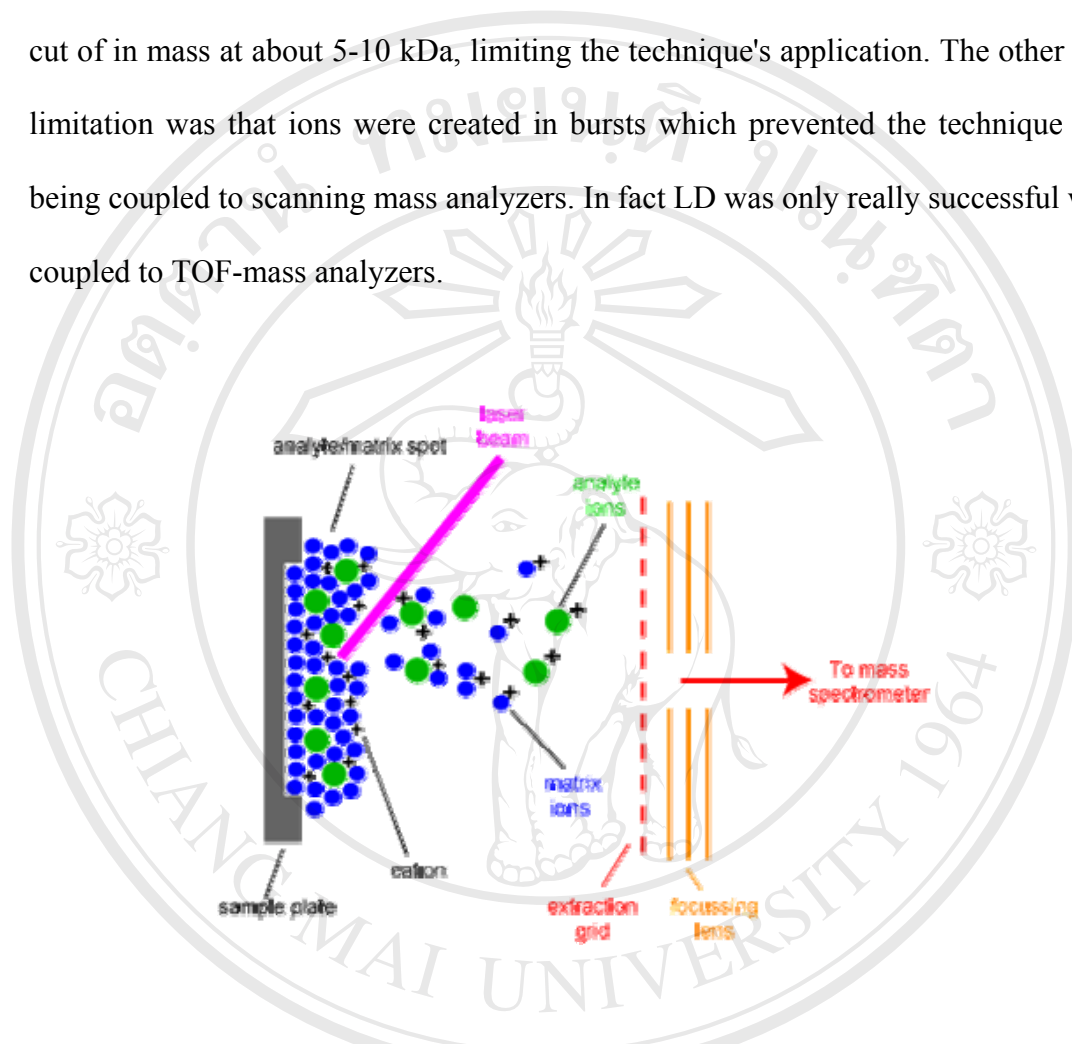


Figure 1.24 A schematic diagram of the mechanism of MALDI.⁴⁶

The mechanism of MALDI is believed to consist of three basic steps:

(I) Formation of a 'solid solution' It is essential for the matrix to be in excess thus leading to the analyte molecules being completely isolated from each other.

This eases the formation of the homogenous 'solid solution' required to produce a stable desorption of the analyte.

(II) Matrix Excitation: The laser beam is focused onto the surface of the matrix-analyte solid solution. The chromophore of the matrix couples with the laser frequency causing rapid vibrational excitation, bringing about localized disintegration of the solid solution. The clusters ejected from the surface consist of analyte molecules surrounded by matrix and salt ions. The matrix molecules evaporate away from the clusters to leave the free analyte in the gas-phase.

(III) Ionization of analyzed: The photo-excited matrix molecules are stabilized through proton transfer to the analyte. Cation attachment to the analyte is also encouraged during this process. It is in this way that the characteristic $[M+X]^+$ ($X = H, Na, K$ etc.) analyte ions are formed. These ionization reactions take place in the desorbed matrix-analyte cloud just above the surface. The ions are then extracted into the mass spectrometer for analysis.

Atmospheric-pressure ionization

Two different sample introduction approaches are used in combination with atmospheric pressure ionization (API) device (**Figure 1.25**). They primarily differ in the nebulization principle and in the application range they cover. In a heated (quartz or stainless steel) tube, where the solvent evaporation is almost completed. Atmospheric pressure chemical ionization (APCI) (**Figure 1.27**), initiated by electrons from a corona discharge needle, is achieved in the same region. Subsequently, the ions generated are sampled into the high vacuum of the mass spectrometer for mass analysis. The solvent emerging from the capillary breaks into fine threads which subsequently disintegrate in small droplets. In some designs, the electrospray

nebulization is assisted by pneumatic nebulization. Such an approach is called an ionspray interface.

Electrospray ionization (ESI)

In electrospray ionization the analyte is introduced to the source at flow rates typically of the order of $1\ \mu\text{l}\ \text{min}^{-1}$. The analyte solution flow passes through the electrospray needle that has a high potential difference (with respect to the counter electrode) applied to it (typically in the range from 2.5 to 4 kV). This forces the spraying of charged droplets from the needle with a surface charge of the same polarity to the charge on the needle. The droplets are repelled from the needle towards the source sampling cone on the counter electrode. As the droplets traverse the space between the needle tip and the cone, solvent evaporation occurs. This is circled on **Figure 1.25** and enlarged upon in **Figure 1.26**. As the solvent evaporation occurs, the droplet shrinks until it reaches the point that the surface tension can no longer sustain the charge (the Rayleigh limit) at which point a "*Coulombic explosion*" occurs and the droplet is ripped apart. This produces smaller droplets that can repeat the process as well as naked charged analyte molecules. These charged analyte molecules (they are not strictly ions) can be singly or multiply charged. This is a very soft method of ionization as very little residual energy is retained by the analyte upon ionization. It is the generation of multiply charged molecules that enables high molecular weight components such as proteins to be analyzed since the mass range of the mass spectrometer is greatly increased since it actually measures the *mass to charge ratio* (m/z) rather than mass *per sec*. The major disadvantage of the technique is that very

little (usually no) fragmentation is produced although this may be overcome through the use of tandem mass spectrometric techniques such as MS/MS or MSⁿ.⁴⁷

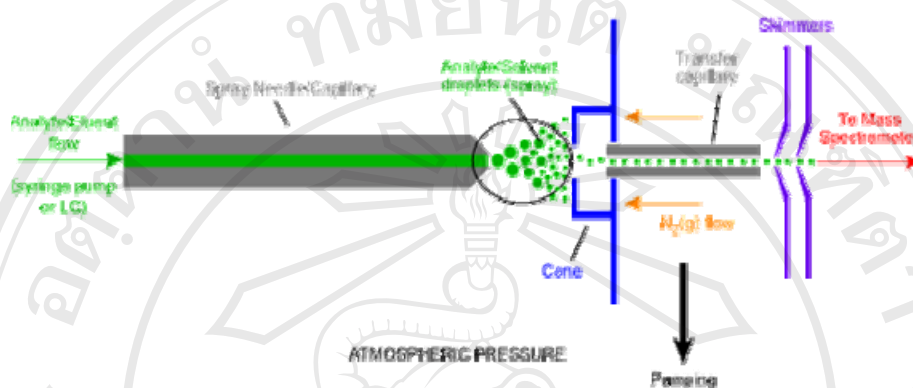


Figure 1.25 A schematic of an ESI interface.⁴⁷

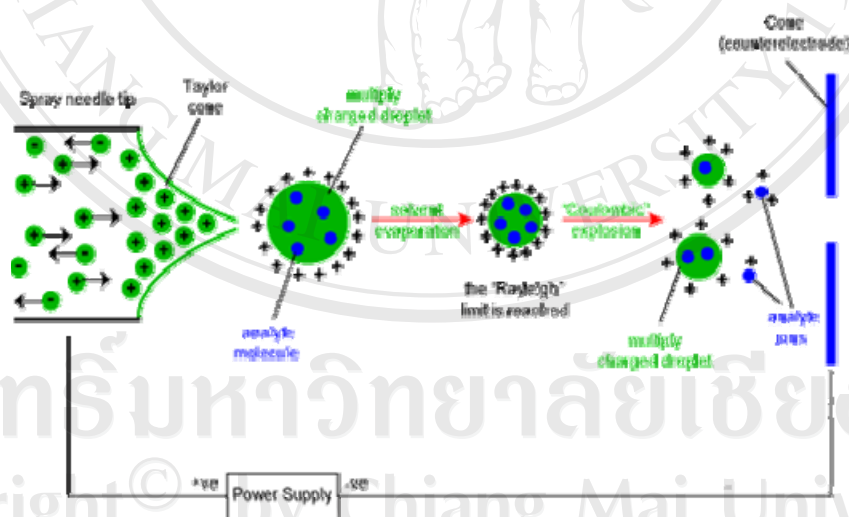


Figure 1.26 A schematic of the mechanism of ion formation in ESI interface.⁴⁷

Many researchers have used electro-spray ionization to investigate anthocyanins in plants, for example, the study of Wu and Prior⁴⁸ that applied HPLC–ESI coupled with DAD to the analysis of anthocyanins in common foods in the United States. Only six common anthocyanidins (delphinidin, cyanidin, pelargonidin, petunidin, peonidin, and malvidin) were found. Anthocyanins in certain vegetables such as red cabbage and red radish were highly conjugated with sugars and acylated groups, and thus, their structures were very complicated. Eight different either aliphatic or aromatic acylated groups (acetoxy, coumaroyl, malonyl *p*-hydroxybenzoyl, feruoyl, caffeoyl, sinapoyl, and oxaloyl) were identified in the anthocyanins. In addition to glucose, six other sugar moieties (galactose, xylose, rhamnose, rutinose, sambubiose, and laminaribiose) were observed. Three varieties of sorghum were found to contain 3-deoxyanthocyanidins and their derivatives as major anthocyanins. Alcalde-Eona and co-workers⁴⁹ employed a HPLC-DAD and ESI-MS techniques to identify the anthocyanins of the coloured tubers of *Oxalis tuberosa*, the second most cultivated tuber in the Andean region. Malvidin glucosides (malvidin 3-*O*-glucoside and 3,5-*O*-diglucoside), 3,5-*O*-diglucosides of petunidin and peonidin, and 3-*O*-glucosides of delphinidin, petunidin and peonidin were found. Only malvidin-3-*O*-acetylglucoside-5-*O*-glucoside was found as an acylated anthocyanin.

Atmospheric pressure chemical ionization (APCI)

Atmospheric pressure chemical ionization (APCI) is an analogous ionization method to chemical ionization (CI). The significant difference is that APCI occurs at atmospheric pressure and has its primary applications in the areas of ionization of low mass compounds. APCI is not suitable for the analysis of thermally labile compounds. The general source set-up (see **Figure 1.27**) shares a strong resemblance to ESI. Where APCI differs to ESI, is in the way ionization occurs. In ESI, ionization is brought about through the potential difference between the spray needle and the cone along with rapid but gentle desolvation. In APCI, the analyte solution is introduced into a pneumatic nebulizer and desolvated in a heated quartz tube before interacting with the corona discharge creating ions. These primary ions collide with the vaporized solvent molecules to form secondary reactant gas ions e.g. H_3O^+ and $(\text{H}_2\text{O})_n\text{H}^+$ (see **Figure 1.28**). These reactant gas ions then undergo repeated collisions with the analyte resulting in the formation of analyte ions. The high frequency of collisions results in a high ionization efficiency and thermalization of the analyte ions. These results in spectra of predominantly molecular species and adduct ions with very little fragmentation. Once the ions are formed, they enter the pumping and focusing stage in much the same as ESI.

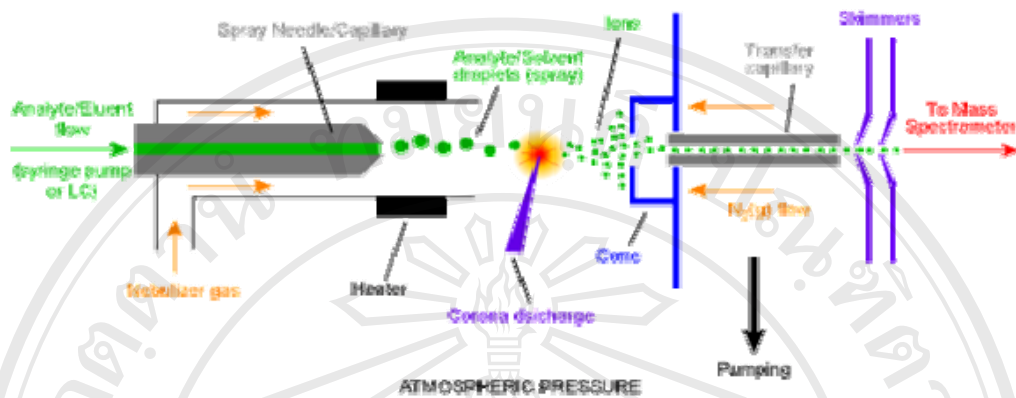


Figure 1.27 A schematic of the components of an APCI source. 47

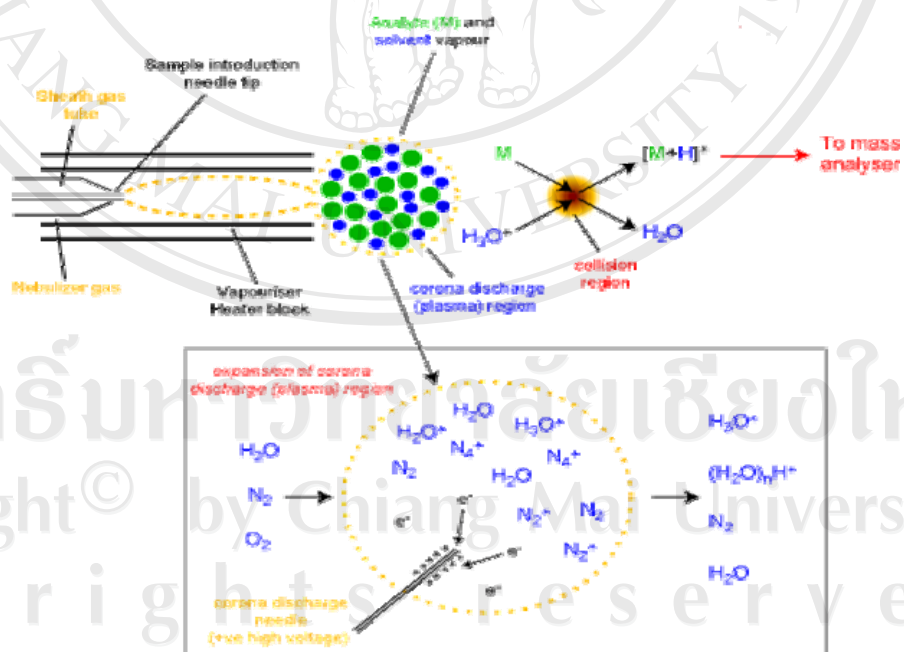


Figure 1.28 A schematic of more detailed view of the mechanism of APCI. 47

All ions in an ionization chamber are to be analyzed according to m/z . Ions have an electrical charge that permits them to be controlled by various electrical fields. They are then, separated by their m/z values in a mass analyzer. Combination with chromatography requires a mass spectrometer that can produce mass spectra at a rapid rate, such as the ion-trap, quadrupole, or time of flight (TOF) mass spectrometers.

Ion trap mass spectrometer

A schematic of the basic set up of a quadrupole ion trap (QIT) mass analyzer is shown in **Figure 1.29**. The ions, produced in the source of the instrument, enter into the trap through the inlet and are trapped through action of the three hyperbolic electrodes; the ring electrode and the entrance and exit end cap electrodes. Various voltages are applied to these electrodes which results in the formation of a cavity in which ions are trapped. The ring electrode RF potential, an A.C. potential of constant frequency but variable amplitude, produces a 3D quadrupolar potential field within the trap. This traps the ions in a stable oscillating trajectory. The exact motion of the ions is dependent on the voltages applied and their individual m/z ratios. For detection of the ions, the potentials are altered to destabilize the ion motions resulting in ejection of the ions through the exit end cap. The ions are usually ejected in order of increasing m/z by a gradual change in the potentials. This stream of ions is focused onto the detector of the instrument to produce the mass spectrum.

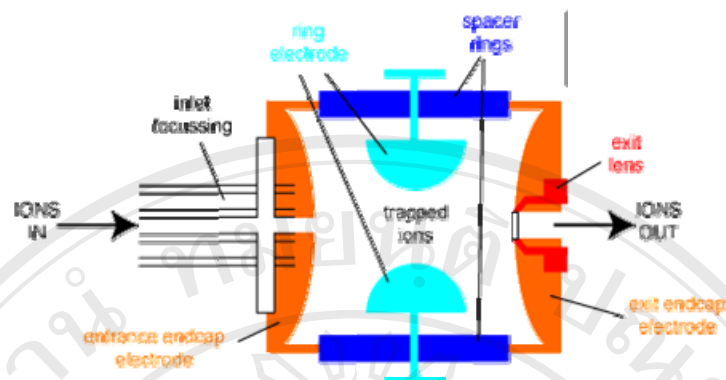


Figure 1.29 A schematic of a quadrupole ion trap mass analyzer.⁵⁰

The nature of trapping and ejection makes a quadrupolar ion trap especially suited to performing MSⁿ experiments in structural elucidation studies. It is possible to selectively isolate a particular m/z in the trap by ejecting all the other ions from the trap. Fragmentation of this isolated precursor ion can then be induced by CID experiments. The isolation and fragmentation steps can be repeated a number of times and is only limited by the trapping efficiency of the instrument.

Sector mass spectrometer

The sector mass spectrometer is one of the most common types of mass analyzer and probably the most familiar to the everyday scientist. In the 1950's, the first commercial mass spectrometers were sector instruments. They consist of some combination of a large electromagnetic (B sector) and some kind of electrostatic focusing device (E sector) (different manufactures use differing geometries).

Figure 1.30 shows a schematic of a standard BE geometry double focusing instrument that is a dual sector instrument consisting of a magnetic sector followed by an electrostatic sector.

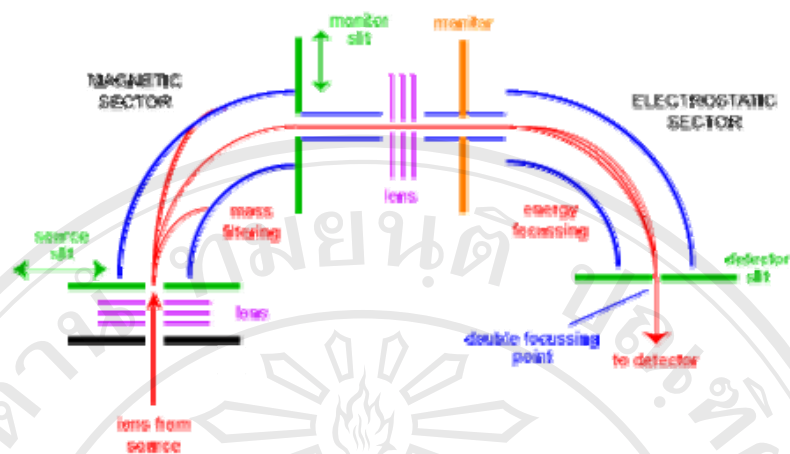


Figure 1.30 A schematic of a sector mass spectrometer.⁵¹

Ions enter the instrument from the source (bottom left) where they are initially focused. They enter the magnetic sector through the source slit where they are deflected according to the left-hand rule. Higher-mass ions are deflected less than lower-mass ions. Scanning the magnet enables ions of different masses to be focused on the monitor slit. At this stage, the ions have been separated only by their masses. To obtain a spectrum of good resolution where all ions with the same m/z appear coincident as one peak in the spectrum, ions have to be filtered by their kinetic energies. After another stage of focusing, the ions enter the electrostatic sector where ions of the same m/z have their energy distributions corrected for and are focused at the double focussing point on the detector slit.

Quadrupole mass spectrometer

A quadrupole mass analyzer consists of four parallel rods (see **Figure 1.31**) that have fixed DC and alternating RF potentials applied to them. Ions produced in the source of the instrument are then focused and passed along the middle of the quadrupoles. Their motion will depend on the electric fields so that only ions of a

particular m/z will be in resonance and thus pass through to the detector. The RF is varied to bring ions of different m/z into focus on the detector and thus build up a mass spectrum. The trajectory of the ions through the quadrupole is actually very complex.

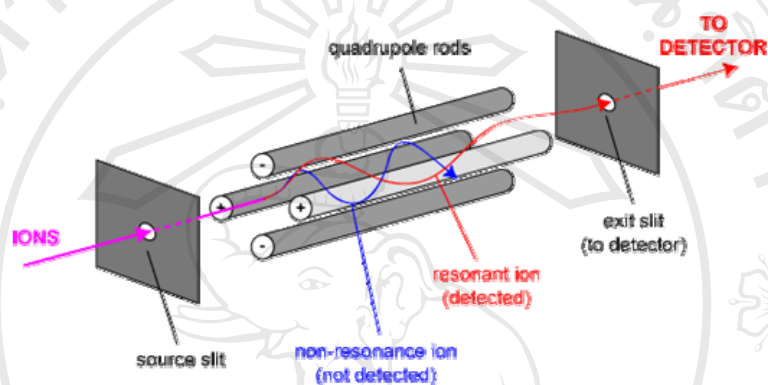


Figure 1.31 Schematic of a quadrupole mass analyzer.⁵²

The two opposite rods in the quadrupole have a potential of $+(U+V\cos(\theta t))$ (labeled + on the **Figure 1.31**) and the other two $-(U+V\cos(\theta t))$ where U is the fixed potential and $V\cos(\theta t)$ is the applied RF of amplitude V and frequency θ . The applied potentials on the opposed pairs of rods varies sinusoidally as $\cos(\theta t)$ cycles with time t . This results in ions being able to traverse the field free region along the central axis of the rods but with oscillations amongst the poles themselves. These oscillations result in complex ion trajectories dependent on the m/z of the ions. Specific combinations of the potentials U and V and frequency will result in specific ions being in resonance creating a stable trajectory through the quadrupole to the detector. All other m/z values will be non-resonant and will hit the quadrupoles and not be

detected (see **Figure 1.31**). The mass range and resolution of the instrument is determined by the length and diameter of the rods.

Time of flight mass spectrometer

The time of flight (TOF) mass spectrometer involves measuring the time required for an ion to travel from an ion source to a detector located 1-2 m from the source. All the ions receive the same kinetic energy during instantaneous accelerations (e.g. 3000 eV), but because they may have different m/z values, they separate into groups according to velocity (and hence m/z) as they traverse the field-free region between the ion source and detector. The ions sequentially strike the detector in order of increasing m/z value, creating a time-based waveform, or simply a transient. Ions of low m/z reach the detector before those of high m/z because the later have velocity, as indicated schematically in **Figure 1.32**.⁵³

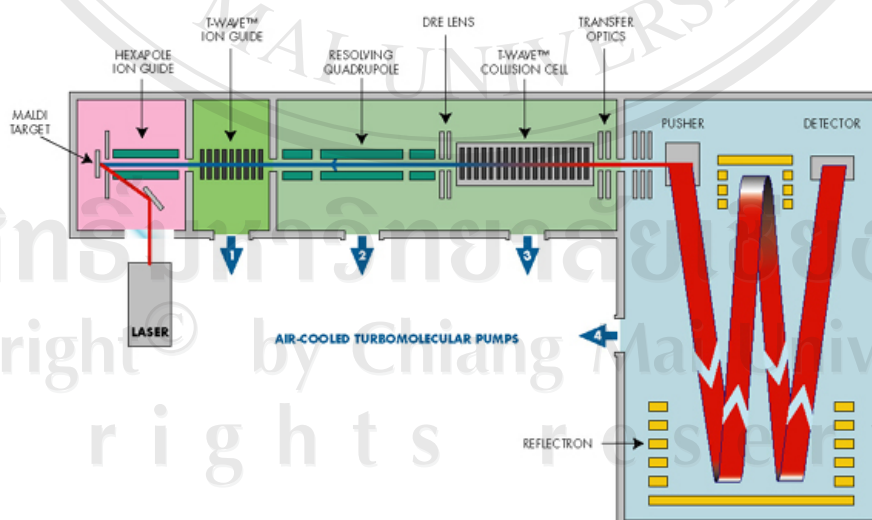


Figure 1.32 Schematic of a TOF mass analyzer.⁵⁴

Mass spectrometry-mass spectrometry

Mass spectrometry-mass spectrometry or tandem mass spectrometry (MS/MS) involves multiple steps of mass selection or analysis, usually separated by some forms of fragmentation. A tandem mass spectrometer is one capable of multiple rounds of mass spectrometry. A conceptual representation of MS/MS is illustrated in **Figure 1.33**. The conventional approach of ionization and fragmentation of a given molecule is represented at the top with mass selection to obtain a conventional mass spectrum. One can then choose ion of a particular (m/z) value as precursor ions for dissociation process for purpose of characterizing the precursor ion. Because of the equipment of two mass selective processes, as illustrated at the top and the bottom of **Figure 1.32**, the name MS/MS was an obvious name for the technology.⁵⁵

A collision cell is a small chamber mounted in the ion path of the mass spectrometry. The collision cell has two small opening, one to let the precursor ions in and the second to let the product ions and surviving precursor ions out. The chamber can be pressurized, usually to 10^{-4} - 10^{-3} torr, with a collision cell is differentially pumped so that the collision gas does not interfere with proper operation of other parts of the mass spectrometer. The collision cell is mounted in an appropriate field-free region that is, between the mass-selective devices.

A precursor ion is any ions selected for analysis by collisionally activated dissociation (CAD). This has been called the parent ion. The precursor ion can be a fragment ion from the first mass spectrometer. A molecular ion also can be chosen as a precursor ion for a CAD experiment. Product ions are those fragment ions produced upon decomposition of a precursor ion in the collision cell during CAD; in the recent past, these were termed daughter ions.

A product ion spectrum is an array of product ions produced by decomposition of a given precursor.

A neutral-loss spectrum is an array of ions that undergo a common loss, such as expulsion of H₂O or glucoside.

Applications of different LC-MS techniques are versatility for the analysis of natural compounds in food. Specific examples of substances are liquid, oligosaccharides, flavonoids, anthocyanins, and related substances. LC-MS is a powerful technique in food analysis and especially for analysis of complex mixtures. The relative applicability of LC-MS techniques is shown in **Figure 1.33**.

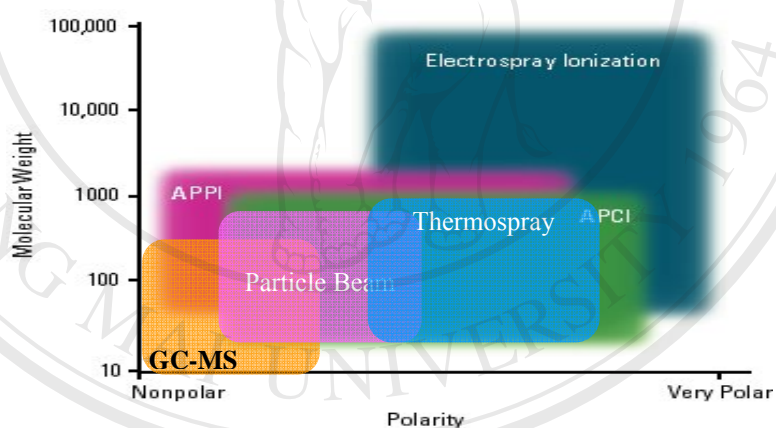


Figure 1.33 Schematic diagram of relative applicability of LC-MS techniques compared with that of GC-MS.

1.4 Fragmentation pathways of anthocyanin glycoside

The major diagnostic fragmentations for anthocyanins identification are those involving the cleavage of two C-C bonds of the C-ring giving two structural informative fragment ions. These ions provide information on the number and type of substituents in A- and B-ring. For free aglycone, the ^{ij}A and ^{ij}B labels refer to the fragments containing intact A- and B-rings, respectively, in which the superscripts i and j indicate the C-ring bonds that have been broken.

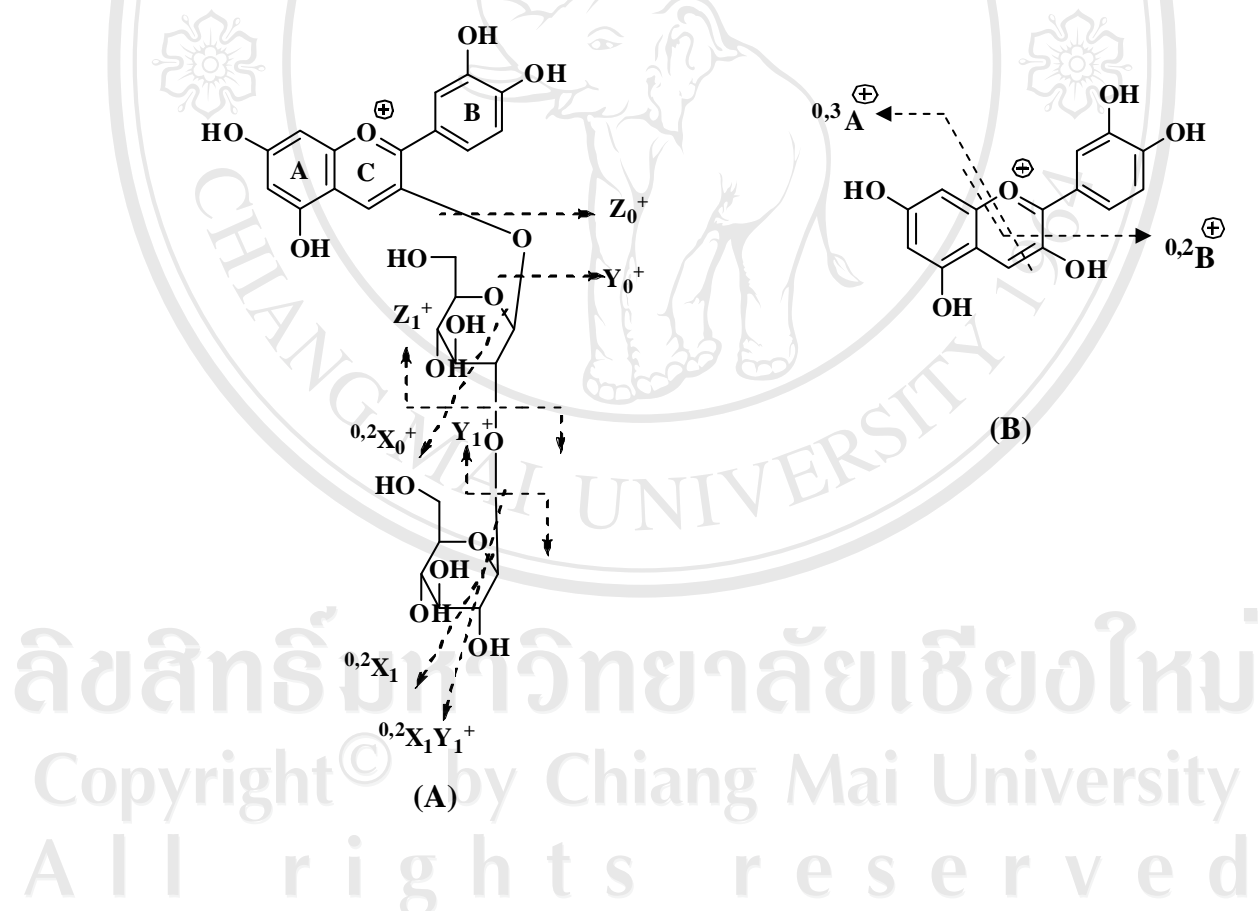


Figure 1.34 Ion nomenclature adopted for anthocyanin glycosides fragmentation

(A) anthocyanin glycoside (B) anthocyanidin aglycone.

For anthocyanin glycosides, the classical nomenclature proposed by Domon and Castell for glycoconjugates was adopted to designate the fragmentations: $^{k,l}X_j$, Y_j , Z_j represents the ions still containing the aglycone, where j is the number of the interglycosidic bonds broken (counted from the aglycone) and k and l denote the cleavage within the carbohydrate (**Figure 1.34**). Differentiation between *O*-glycoside, *C*-glycosides and *O,C*-glycoside can be made by examining the first-order positive ion spectra or low-energy CID spectra. The protonated *O*-glycoside gives rise to Y_1^+ and Y_0^+ ions which are formed by rearrangement reactions at the interglycosidic bonds without cross-ring cleavage of the carbohydrate molecules. In the case of *O,C*-diglycosides, only Y_1^+ ions, formed by fragmentation at the interglycosidic linkage, are detected. Whereas in the case of *C*-glycoside, only $[M+H]^+$ ions are observed together with cross-ring cleavages of the saccharidic residue and the loss of molecular of water.

Anthocyanins *O*-glycosides

Mass spectrometric method can be used to obtain information on the carbohydrate sequence and the aglycone moiety. In many cases, the glycosylation position, the interglycosidic linkage position and the stereochemical identity of the terminal sugar residue can be defined. Cleavage at the glycosidic *O*-linkages with a concomitant H-rearrangement leads to the elimination of monosaccharide residues, such as loss of hexose (162 Da), deoxyhexose (146 Da), and pentose (132 Da) allowing the determination of the carbohydrate sequence (**Figure 1.35**).

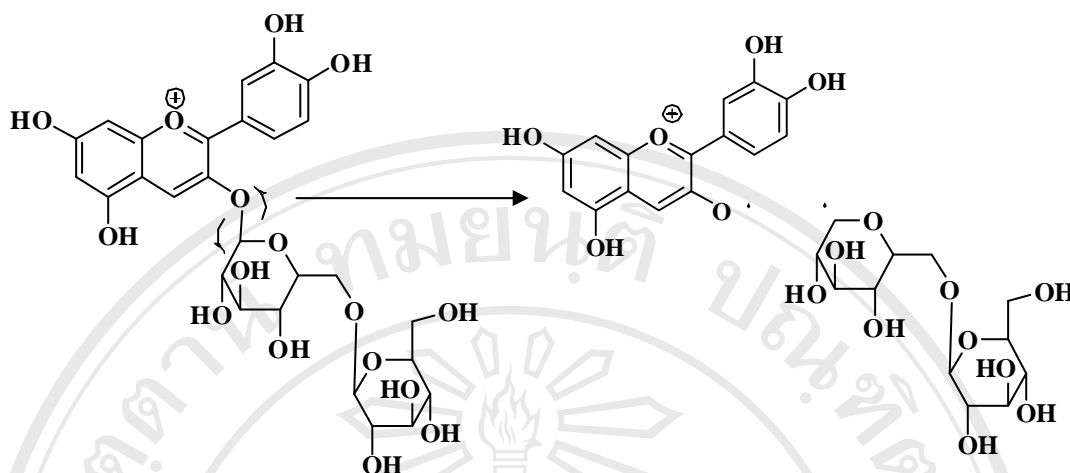


Figure 1.35 Formation of the radical aglycone product ion (Y_0^+) by a hemolytic cleavage of the glycosidic bond between the aglycone and the glycan residue.

Anthocyanin C-glycosides

In anthocyanin C-glycosides, the sugar is directly linked to the anthocyanin nucleus via an acid-resistant C-C bond. Therefore, the first-order mass spectra provide limited structural information except for the molecular mass. MS/MS analysis in combination with CID allows the characterization of C-glycoside in both the negative and positive ion mode. The major fragmentation pathways concern cross-ring cleavages of the saccharidic residue as shown in **Figur 1.36**. C-linked sugars have only been found at the C-6 and C-8 position of the anthocyanins.

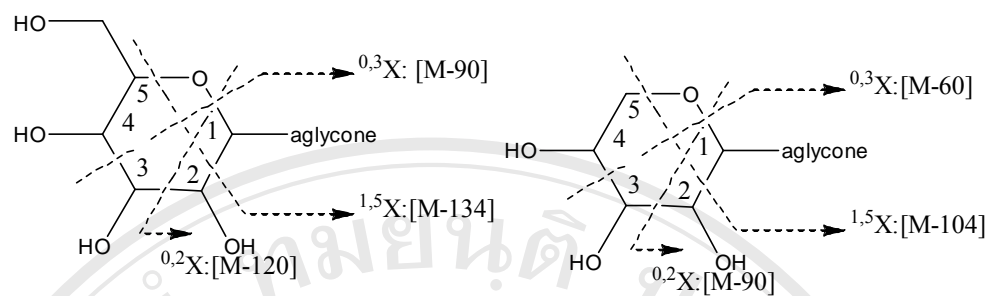


Figure 1.36 Characteristic product ions formed by cross-ring cleavage in a hexose and pentose residue.

Anthocyanins-3-*O*-diglucoside and Anthocyanins-3-*O*-glucoside-5-*O*-glucoside

Mass spectrometric method can also be used to obtain information on the *O*-diglycosyl and di-*O*-glycosyl anthocyanins. When an anthocyanidin substituted with two sugars in positions 3 and 5, the fragmentation of the molecular ion leads to the formation of three fragment ions, one corresponds to the aglycone, another to the 3-*O*-glucoside and the last to the 5-*O*-glucoside. If both sugars are the same, only two signals would appear in the mass spectrum, one corresponding to the aglycone and the other corresponds to the two possible monoglucosides. Whereas an anthocyanin with 1-2 interdiglycosidic linkage, the fragmentation of the molecular ion leads to the $^{0,2}X_0^{0,2}X_1^+$ and $^{0,2}X_0Y_1^+$. These ions can be considered as characteristic of the 1-2 interglycosidic linkage in the anthocyanidins. Additionally the ions at $[Y_1^+ - 2H_2O]$, $[Y_1^+ - 3H_2O]$, and $[Y_1^+ - 2H_2O - 60]$, which are also characteristic of anthocyanidin-*O*-diglucoside were observed. The formation of Z_1^+ ion are useful for establishing that the eliminated and terminal carbohydrate unit is linked to another carbohydrate and not directly to the aglycone, thus useful for the differentiation of *O*-diglycosyl and di-*O*-glycosyl anthocyanins.⁵⁶

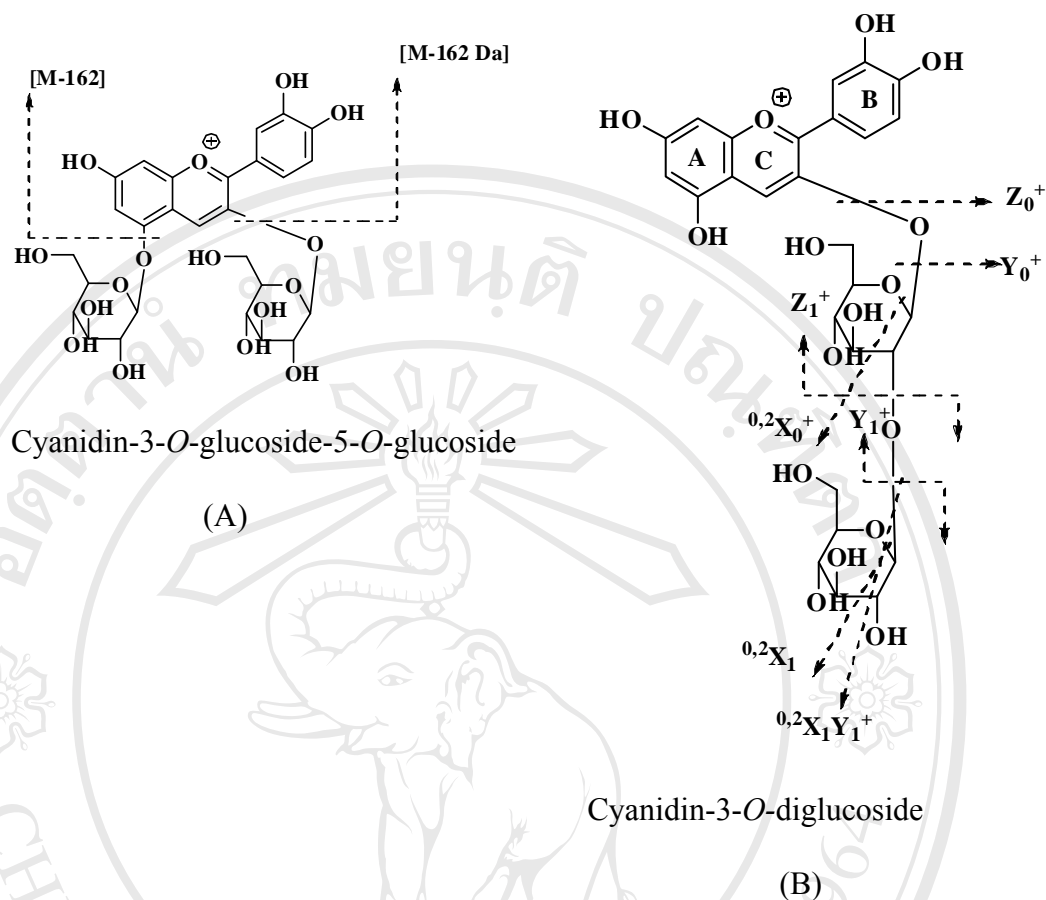


Figure 1.37 Characteristic product ions formed by (A) di-*O*-glucoside and (B) diglucoside anthocyanins.

Many researchers have applied the LC-MS and MS/MS techniques to analysis and identification of anthocyanins in fruits, flowers and other plants. Seeram and co-workers⁵⁷ analyzed phenolic compounds in strawberry fruit powder and strawberry fruit extracts using LC-ESI-MS. Phenolics identified included ellagic acid (EA), EA-glycosides, ellagitannins, gallotannins, anthocyanins, flavonols, flavanols and coumaroyl glycosides. The anthocyanidins were pelargonidin and cyanidin, found predominantly as their glucosides and rutinosides. The major flavonol aglycons were quercetin and kaempferol found as their glucuronides and glucosides.

Tian and co-workers⁵⁸ developed a systematic method for anthocyanin identification using (MS/MS) coupled to HPLC with PDA. Scanning for the precursors of commonly found anthocyanidins (cyanidin, delphinidin, malvidin, pelargonidin, petunidin, and peonidin) using LC-MS/MS on a triple quadrupole instrument allows for the specific determination of each category of anthocyanins. Further characterization of each anthocyanin was performed using MS/MS product-ion analysis, common-neutral-loss analysis, and selected reaction monitoring (SRM) technique. The method was demonstrated for analysis of anthocyanins in black raspberries, red raspberries, highbush blueberries, and grapes (*Vitis vinifera*). In some previous reports anthocyanins in black raspberries and red raspberries were confirmed and characterized. Common-neutral-loss analysis allows for the distinction of anthocyanin glucosides or galactosides and arabinosides in highbush blueberries. Separation and identification of anthocyanin glucosides and galactosides were achieved using LC-MS/MS with SRM. Anthocyanin isomers such as cyanidin sophoroside and 3,5-diglucoside were differentiated by their fragmentation pattern during product-ion analysis. Fifteen anthocyanins (all possible combinations of five anthocyanidins and three sugars) were characterized in highbush blueberries. Pelargonidin-3-glucoside and pelargonidin-3,5-diglucoside were detected and characterized for the first time in grapes. The present approach allows mass spectrometry to be used as a highly selective detector for rapid identification and characterization of anthocyanins and can be used as a sensitive procedure for screening anthocyanins in fruits and vegetables.

Revilla and co-workers⁵⁹ studied the MS detection for analysis and identification of anthocyanins by LC–MS. The anthocyanin composition of different red grape skin extracts and commercial monovarietal wines were determined. Results showed that some of these derivatives were present in grape and young wine. The combination of diode array detection and MS analysis was demonstrated to be essential for identification of these anthocyanin derivatives.

Edy Sousa De Brito and co-workers⁶⁰ identified and quantified flavonoids in cashew apple by LC-DAD-ESI-MS. One anthocyanin and thirteen glycosylated flavonols were detected in a methanol–water extract. The 3-*O*-galactoside, 3-*O*-glucoside, 3-*O*-rhamnoside, 3-*O*-xylopyranoside, 3-*O*-arabinopyranoside and 3-*O*-arabinofuranoside of quercetin and myricetin, and kaempferol-*O*-glucoside were identified by direct comparison with standards or previously identified flavonoids in cranberry. The anthocyanin was a 3-*O*-hexoside of methyl-cyanidin.

Montoro and co-workers⁶¹ identified and quantified anthocyanins in berries of *Myrtus communis*, which prepared following a typical Sardinia myrtle liqueur recipe by HPLC coupled with ESI-MS/MS using, respectively, an ion trap and a triple quadrupole mass analyzer. Five anthocyanin glucosides and four anthocyanin arabinosides were found.

Nielsen and co-workers⁶² identified 3,5-*O*-D-diglucosides of pelargonidin, cyanidin, peonidin, delphinidin, petunidin and malvidin in orange, pink, red and magenta flowers. Pink, red and magenta varieties contained relatively high amounts of quercetin based flavonols. Four quercetin flavonols were identified, namely quercetin-3-*O*-D-glucoside and three that were quercetin-3-*O*-L-rhamnoside based, with either glucose, xylose or arabinose attached to position 2 of the rhamnose.

In addition, the presence of at least three kaempferol based diglycosides was suggested from LC–MS analyses.

Kazuma and co-workers⁶³ investigated flavonoids in the petals with different petal colors by using LC-MS/MS. Delphinidin-3-*O*-(2-*O*- α -rhamnosyl-6-*O*-malonyl)-glucoside was a newly isolated compound of the petals of a mauve line together with three known anthocyanins. They were identified structurally using UV, MS, and NMR spectroscopy.

Wu and coworkers⁶⁴ developed and validated the LC–ESI-MS method for the identification and determination of seven flavonoids, namely, epimedin A, epimedin B, epimedin C, icariin, sagittatoside B, 2-*O*-rhamnosyl icariside II, and baohuoside I in epimedium from different sources.

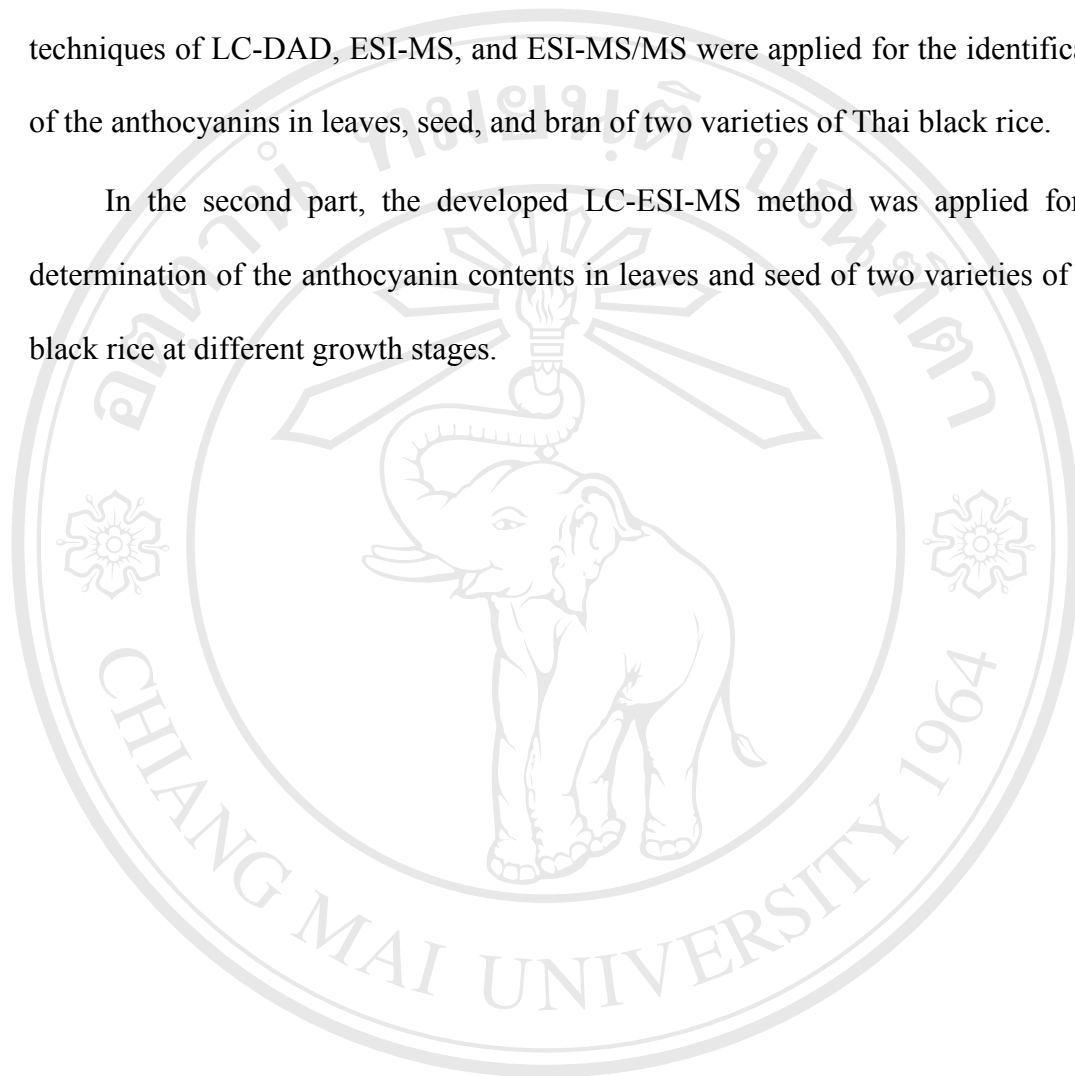
Arapitsas and co-workers⁶⁵ analyzed and identified anthocyanins in red cabbage using HPLC-DAD-ESI-Qtrap-MS. Twenty four anthocyanins were separated and identified, all having cyanidin as aglycon, represented as mono-, di-glycoside, and acylated, with aromatic and aliphatic acids. Nine anthocyanins were identified for the first time in red cabbage.

Monagas and co-workers⁶⁶ identified grape anthocyanins (delphinidin, cyanidin, petunidin, peonidin and malvidin-3-glucosides, -3-(6-acetyl)-glucosides and -3-(6-*p*-coumaroyl)-glucosides, peonidin and malvidin-3-(6-caffeoyl)-glucosides) and anthocyanin-derived pigments (the pyruvate, vinylcatechol, vinylepicatechin, vinylphenol and vinylguaiacol derivatives of malvidin-3-glucoside, and malvidin-3-(6-acetyl)-glucoside-vinylepicatechin) using LC-MS/MS.

1.5 Aims of This Research

In this study, the experiment was separated into two parts. In the first part, the techniques of LC-DAD, ESI-MS, and ESI-MS/MS were applied for the identification of the anthocyanins in leaves, seed, and bran of two varieties of Thai black rice.

In the second part, the developed LC-ESI-MS method was applied for the determination of the anthocyanin contents in leaves and seed of two varieties of Thai black rice at different growth stages.



ลิขสิทธิ์มหาวิทยาลัยเชียงใหม่

Copyright© by Chiang Mai University

All rights reserved